https://doi.org/10.5194/egusphere-2025-306
Preprint. Discussion started: 17 February 2025

Extension of the S5P-TROPOMI CCD tropospheric ozone retrieval to mid-latitudes

Swathi Maratt Satheesan[1], Kai-Uwe Eichmann[1], Mark Weber[1], Roeland Van Malderen[2], Ryan Stauffer[3], and David Tarasick[4]

[1]Institute of Environmental Physics, University of Bremen, Bremen, Germany
[2]Royal Meteorological Institute of Belgium, Brussels, Belgium
[3]Earth Sciences Division, NASA/Goddard Space Flight Center, Greenbelt, MD, USA
[4]Environment and Climate Change Canada, Downsview, ON, CA

Correspondence: Swathi Maratt Satheesan (swathi@iup.physik.uni-bremen.de)

Abstract.

Tropospheric ozone, a key atmospheric pollutant and greenhouse gas, exhibits significant spatio-temporal variability on seasonal, inter-annual, and decadal scales, posing a challenge for satellite observation systems. Methods like the Convective Cloud Differential (CCD) and Cloud Slicing Algorithms (CSA) are standard for Tropospheric Column Ozone (TCO) retrievals but are limited to the tropical band (20°S-20°N). This study presents the first successful global application of CCD retrieval outside the tropical region. We introduce the CHORA-CCD (Cloud Height Ozone Reference Algorithm-CCD) for retrieving near-global TCO from TROPOMI. It utilises a local cloud reference sector (CLCD, CHORA Local Cloud Decision) to determine the stratospheric (above cloud) column ozone (ACCO). The ACCO is subtracted from the total column in clear-sky scenes to determine the TCO. The new approach presented here minimises the impact of stratospheric ozone variability, which is generally higher in the extratropics. An iterative approach is used to automatically select an optimal local cloud reference sector around each retrieval grid box, varying the radius from 60 to a maximum of 600 km, for which a mean TCO is determined until a sufficient number of ground pixels with nearly full cloud cover are found. Due to the prevalence of low-level clouds in mid-latitudes, the TCO calculation is constrained to the column from the surface up to the reference altitude of 450 hPa. There are two independent methods used, (I) CLCD-C which uses an ozone climatology and (II) CLCD-T, an alternative method which estimates the ACCO at 450 hPa by linear regression (Theil-Sen) in cases where the cloud-top-heights in the local cloud sector vary sufficiently. The Theil-Sen approach is a combination of the CCD and CSA methods. The CLCD algorithm dynamically decides between the CLCD-C and CLCD-T to determine ACCO depending on the cloud characteristics. The CLCD algorithm is further refined by introducing a homogeneity criterion for total ozone to overcome inhomogeneities in stratospheric ozone. Monthly averaged CLCD TCOs have been determined over the tropics and mid-latitudes (60°S-60°N) using TROPOMI data from 2018 to 2022. The method's accuracy was investigated by comparing spatially collocated SHADOZ/WOUDC/NDACC HEGIFTOM ozonesonde measurements from 36 stations. The validation results reveal that CLCD TCO retrievals are in good agreement with ozonesondes at most stations with an overall statistical bias of 0.6 DU and dispersion of 2.5 DU. Across all stations, the maximum bias and dispersion are around ∼5 DU and 4 DU, respectively. The CLCD approach effectively captures tropospheric ozone enhancements across diverse regions, including Northeast China and North America, with particular

https://doi.org/10.5194/egusphere-2025-306
Preprint. Discussion started: 17 February 2025

sensitivity to areas impacted by significant emission sources. Our results demonstrate the advantage of using the modified local cloud reference sector, providing an important basis for subsequent systematic applications in current and future missions, in particular, geostationary satellites with the emphasis on observing higher latitudes.

1 Introduction

Tropospheric ozone plays a crucial role in Earth's atmosphere, acting as a greenhouse gas at higher altitudes and a component of smog closer to the surface (Crutzen, 2016). The limited lifespan of tropospheric ozone and its significant warming impact underscores the potential for climate and health improvements through precursor emission reduction strategies. It emphasises the necessity for accurate quantitative analysis of tropospheric ozone levels to assist policymakers in developing effective preventive measures (Jaffe et al., 2018).

The Convective Cloud Differential (CCD) method (Ziemke et al., 1998) and the Cloud Slicing Algorithms (CSA) (Ziemke et al., 2005) are two established tropospheric ozone retrieval approaches, currently limited to the tropical band (20°S-20°N). The tropical CCD method has proven its efficacy by application to active satellite sensors, including TOMS, Aura OMI, MetOp GOME-2, and Sentinel-5 Precursor TROPOMI (Valks et al., 2003; Ziemke et al., 2005, 2010; Heue et al., 2016; Leventidou et al., 2016, 2018; Hubert et al., 2021; Maratt Satheesan et al., 2024). Ziemke et al. (2005) highlighted the possibility of extending the CCD method to higher latitudes. They point out that the determination of stratospheric ozone and, consequently, tropospheric ozone is feasible due to the presence of highly reflective clouds across all latitudes over the Pacific region (see also Hu et al., 2020). In their study, the application of the CCD method from TOMS data was expanded over the Pacific region into the mid-latitudes (50°S-60°N) for the time period from 1979 to 2003. In a more recent assessment by Ziemke and Chandra (2012), the performance of the CCD method was evaluated at higher latitudes (60°S-60°N) over the Pacific using Aura OMI and MLS ozone measurements from 2004 to 2010. The zonal invariance of stratospheric ozone, a basic assumption for CCD to work, is not valid outside the tropics, particularly during winter and spring months (Ziemke and Chandra, 2012). Therefore, the applicability of the CCD method outside the tropics has been so far limited to the Pacific region.

We developed an improved version of CHORA (Cloud Height induced Ozone Reference Algorithm) to properly address the issue of greater stratospheric ozone variability outside the tropics (Maratt Satheesan et al., 2024). The original CHORA (Cloud Height induced Ozone Reference Algorithm), an advanced version of the CCD technique developed at IUP Bremen (Leventidou et al., 2016, 2018), builds on the established Pacific cloud reference sector method for tropical tropospheric ozone retrieval (CHORA Pacific Cloud, CPC). Here, the Above Cloud Column (ACCO) or stratospheric column ozone is retrieved over the tropical eastern Indian and western Pacific oceans (70°E–170°W) and then subtracted from clear-sky total ozone (same latitude, but all longitudes) to obtain the tropospheric ozone column (Ziemke et al., 1998; Valks et al., 2003, 2014; Leventidou et al., 2016, 2018; Hubert et al., 2021).

The advanced CLC version (CHORA Local Cloud) uses a local cloud reference sector for ACCO calculation and a total ozone homogeneity criterion (Maratt Satheesan et al., 2024). Furthermore, the CLCT method (CHORA Local Cloud Theil-Sen) has been added to directly enable ACCO retrievals below the reference height of 270 hPa using Theil-Sen linear regression

https://doi.org/10.5194/egusphere-2025-306
Preprint. Discussion started: 17 February 2025

to derive the cloud pressure correction factor, thus replacing the need for an external ozone climatology as used in CLC. CLCT combines the standard CCD with the cloud-slicing approach (Maratt Satheesan et al., 2024).

The upgraded algorithm CLCD (CHORA Local Cloud Decision), designed for near global tropospheric ozone column retrieval (60°S - 60°N), is presented here. The CLCD approach effectively addresses the primary limitations of the scarcity of highly reflective clouds outside tropical regions. The algorithm makes a dynamic decision for ACCO estimation by analysing cloud characteristics and choosing between the CLCD-C (homogeneous cloud cover) and CLCD-T method (variable cloud heights). The CLCD algorithm is further refined by a homogeneity criterion for the total ozone to address the inhomogeneities in stratospheric ozone.

Due to the much higher abundance of low-level clouds in the extratropics, the retrieved tropospheric columns extend from the surface to the reference altitude of 450 hPa (∼5.5 km altitude). This altitude range encompasses a substantial portion of the troposphere, where many dynamic atmospheric processes occur, e.g. long-range transport of boundary layer air to the upper troposphere. Recent studies indicate that a significant stratospheric influence on tropospheric ozone concentrations is observed, particularly within the 1000–450 hPa layer, where seasonal variations reveal enhanced ozone abundances. The analysis by Williams et al. (2019) highlights that the stratospheric contribution to tropospheric ozone at the 450 hPa level is larger than previously understood, estimated to exceed 50 % in wintertime extratropics. The Tropospheric Ozone Assessment Report Phase II, (TOAR-II, https://igacproject.org/activities/TOAR/TOAR-II) also adopts 450 hPa as a reference pressure level because it is a standard atmospheric pressure level commonly utilised in atmospheric studies to denote the lower/mid-troposphere (Jenkins et al., 2012; Pope et al., 2024). The common reference level ensures consistency in data comparison and analyses from various studies.

This paper is structured as follows. The measurement data taken from S5P-TROPOMI used for deriving the tropospheric ozone columns are described in Section 2. Spatially Collocated ozonesonde measurements used as a reference for validation are described in Section 3. The mid-latitude algorithm (CLCD) is explained in Section 4. Section 5 compares tropospheric ozone from the CLCD algorithm with data from 36 ozonesonde stations and tropical CLCT retrievals. Potential sources of biases are discussed. In Section 6, all major findings are recollected and discussed to derive conclusions on the CLCD algorithm's efficiency.

2 Measurement data

2.1 S5p-TROPOMI

The TROPOspheric Monitoring Instrument (TROPOMI), onboard the Copernicus Sentinel-5 Precursor (S5P) satellite, was launched on 13 October 2017 to monitor atmospheric composition. It provides daily global coverage with high spatial resolution of initially 5.5x7 km^2, which was improved to 5.5x3.5 km^2 in August 2019 (Ingmann et al., 2012). TROPOMI retrieves various trace gas columns, clouds, and aerosols. This includes total ozone column and cloud parameters needed for tropospheric ozone retrieval using the CCD method (Ludewig et al., 2020).

https://doi.org/10.5194/egusphere-2025-306
Preprint. Discussion started: 17 February 2025

This study uses five years of reprocessed/offline TROPOMI total ozone column data (processor version 02.04.01 and above) from 1 June 2018 to 31 December 2022. Data was used from the GODFIT algorithm, which is based on ozone absorption in the UV Huggins bands (325-335 nm) (ESA, 2022). Cloud parameters, including cloud fraction and cloud-top-height/pressure, are taken from the OCRA and ROCINN algorithms, respectively (Loyola and Ruppert, 1998; Rodriguez et al., 2007; Maratt Satheesan et al., 2024).

3 Reference data

3.1 Ozonesondes

Ozonesondes, widely recognised as a primary and precise ground-based method for measuring vertical ozone profiles, are deployed across numerous stations worldwide. Covering the surface to the middle stratosphere (∼30–35 km) with an impressive vertical resolution of 100 - 150 m, ozonesondes play a crucial role in capturing atmospheric information.

ECC-type sondes stand out for their enhanced performance in the troposphere, showcasing a bias of ±5–7% and a precision of 3–5% (Hubert et al., 2016). Their capability to provide detailed and accurate vertical ozone profiles makes them well-suited for verifying and improving the reliability of satellite data (Huang et al., 2017; Hubert et al., 2021; Tarasick et al., 2021; Keppens et al., 2024).

In order to validate our results, we rely on ozonesonde data obtained from three different sources: the Network for the Detection of Atmospheric Composition Change (NDACC, http://www.ndacc.org), World Ozone and Ultraviolet Radiation Data Centre (WOUDC, http://www.woudc.org), and the Southern Hemisphere ADditional OZonesondes network (SHADOZ, https://doi.org/10.57721/SHADOZ-V06) (Thompson et al., 2019; Sterling et al., 2018; Thompson et al., 2021). These ozone profile data have been homogenized within the framework of the TOAR-II (2020-2024) Focus Working Group HEGIFTOM (Harmonization and Evaluation of Ground-based Instruments for Free Tropospheric Ozone Measurements) and were obtained here from twenty-six stations from the websitehttps://hegiftom.meteo.be/datasets/ozonesondes. The aim of homogenizing ozonesonde profiles is twofold. First, it corrects biases related to instrumental factors, such as sonde type and sensing solution strength. This correction reduces overall uncertainty from 10–20% to 5–10%. Second, it provides an uncertainty estimate for each ozone partial pressure measurement in the profile. This approach enhances the reliability of ozonesonde data and allows for more accurate assessments of atmospheric ozone levels (Smit and Thompson, 2021).

The screened ozonesonde volume mixing ratio profiles at each station are integrated from the initial measurement level up to 450 hPa (≈ 5.5 Km), yielding the tropospheric ozone sub column, which is then compared with TROPOMI CLCD data. The conversion of ozone volume mixing ratio profiles to columns in Dobson Units (DU) is conducted using the same method as outlined in Maratt Satheesan et al. (2024). Ozonesonde profiles are considered spatially collocated with satellite data when the station falls within the grid box of the retrieved TROPOMI tropospheric ozone column, which is typically $0.5^\circ \times 0.5^\circ$.

In total, sub-columns from thirty-six ozonesonde stations (nine in the tropics, four in the subtropics and nineteen at mid-latitudes) were compared with spatially collocated TROPOMI tropospheric ozone columns from June 2018 to December 2022. The station locations are displayed in Fig.1.

https://doi.org/10.5194/egusphere-2025-306
Preprint. Discussion started: 17 February 2025

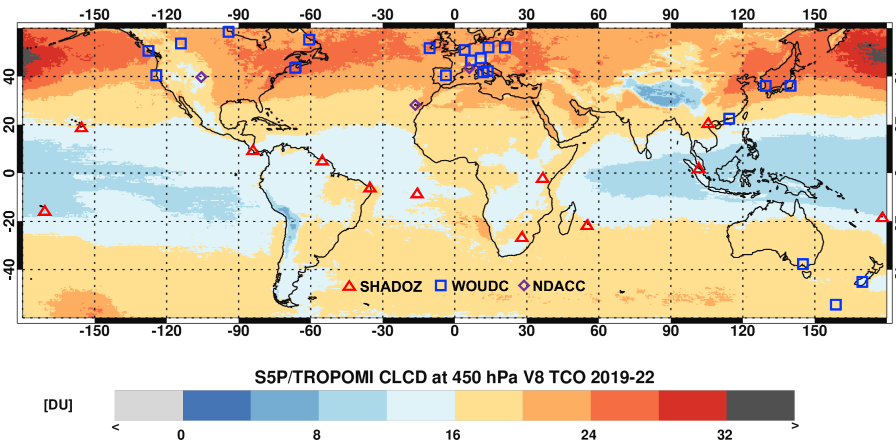

Figure 1. Distribution of SHADOZ/WOUDC/NDACC ozonesonde stations. The colour map shows the four-year mean TROPOMI tropospheric ozone column [DU] from the surface to 450 hPa (2019-2022) retrieved with CLCD.

4 Methodology

4.1 CHORA Local Cloud Decision (CLCD) algorithm

The basic idea of CCD is to subtract the mean above-cloud-column ozone (ACCO) from a cloud reference sector from the mean clear-sky total ozone in a grid box to obtain the tropical column ozone amount in that grid box. The advanced CLCD algorithm combines both the local cloud algorithms CLC and CLCT as described in Maratt Satheesan et al. (2024). In this advanced approach for mid-latitudes, both CLC and CLCT algorithms are updated with different cloud selection criteria. These optimized versions are referred to as CLCD-C and CLCD-T, respectively.

The CLCD-C method uses a global ozone profile climatology to adjust each ACCO of the cloud reference sector to a common reference altitude, here 450 hPa, before taking the mean. We use the TOMS V8 ozone profile climatology, an extension of the NASA Goddard Space Flight Center (GSFC) climatology. It provides total ozone classified ozone profiles in 10° wide latitude bands for each month (McPeters et al., 2003).

The CLCD-T approach determines the mean ACCO at the reference altitude by using Theil-Sen regression. ACCO is a function of cloud-top-pressure. The regression directly interpolates to the reference pressure level avoiding the use of an ozone climatology. The regression is also used to determine the average ozone volume mixing ratio in the layer between the lowest and highest CTP from the slope of the regression line, as done in the cloud-slicing algorithm (CSA) (Ziemke et al., 2001).

The local cloud reference sector selection has been modified compared to the tropical algorithms. An optimal circular local cloud reference sector around the centre of each retrieval grid box is iteratively adjusted by varying the radius between 60 and 600 km until the number of cloudy ground pixels (with a minimum cloud fraction of 0.8 and cloud-top-height greater than 2 km) exceeds 20. The choice of a circular reference sector in the extratropics is influenced by varying wind directions, which

https://doi.org/10.5194/egusphere-2025-306
Preprint. Discussion started: 17 February 2025

result in no single dominant direction, unlike in the tropics, where winds primarily follow an east-west pattern. Additionally, the smaller ground coverage of geostationary satellites in these regions makes a longitudinally varying cloud sector less practical. This approach ensures more effective sampling by accommodating the dynamic wind conditions.

In the tropical algorithms, the cloud sector was iteratively adjusted only in longitudinal directions (Maratt Satheesan et al., 2024). Due to the high occurrence rate of low-level clouds in the extratropics, the common reference level or upper altitude limit for the tropical ozone column is 450 hPa (∼5.5 Km) instead of 270 hPa.

The CLCD algorithm dynamically decides between the CLCD-C and CLCD-T for deriving the mean ACCO by analysing cloud characteristics (Fig.3). It examines cloud-top-heights by computing their standard deviation (2σ) within the reference sector. Clouds above 6 km are identified as high clouds and between 2 and 6 km as low-level clouds. If the standard deviation of CTH exceeds 2 km, clouds are considered variable and suitable for Theil-Sen regression (CLCD-T). Otherwise, the clouds are considered homogeneous, and the ozone climatology is used in the ACCO calculation (CLCD-C). Quality flags from 1 to 4 are assigned to tropospheric ozone columns based on the range and variability of cloud-top-heights observed in the reference sector. The CLCD-C method is chosen for homogeneous CTH (quality flags 1 in case of low or 3 in case of high clouds). In contrast, the Theil-Sen method (CLCD-T) is applied to variable CTH (quality flags 2 or 4 in case of low and high clouds, respectively) (Fig.4).

The choice between the CLCD-C and CLCD-T algorithms is determined solely by cloud variability, with CLCD-C performing better in cases of low variability and CLCD-T excelling when cloud variability is higher. While higher clouds in the tropics necessitate larger corrections to the 450 hPa reference altitude, our primary focus is on tropospheric ozone retrievals over mid-latitudes, where low-level clouds dominate, and smaller corrections to the reference altitude are expected. Analysis of Figure 4 confirms that more than 65% of clouds in these regions are low-level with uniform top heights, making the CLCD-C method more suitable for latitudes above 20°.

Subsequently, total ozone (TOZ) under clear sky conditions ($CF \leq 0.2$) is daily averaged for each $0.5° \times 0.5°$ grid box. In the final step, the tropospheric ozone column in each grid box is determined by subtracting the mean ACCO from the total ozone. In rare instances where the computed tropospheric ozone value turns out to be negative, it is substituted with a designated fill value and assigned quality flag of 5.

The CLCD algorithm is further refined by introducing a homogeneity criterion for total ozone. This filtering addresses inhomogeneities in stratospheric ozone. TCO is computed only when the standard deviation (1σ) of the total ozone column under cloudy conditions ($CF \geq 0.8$) from the local cloud reference sector is less than 10 DU; otherwise, it is replaced with a fill value and assigned the quality flag of 5.

The main differences between the mid-latitude algorithm CLCD and the tropical algorithms (CLC and CLCT) lie in their cloud selection criteria and the climatology used.

https://doi.org/10.5194/egusphere-2025-306
Preprint. Discussion started: 17 February 2025

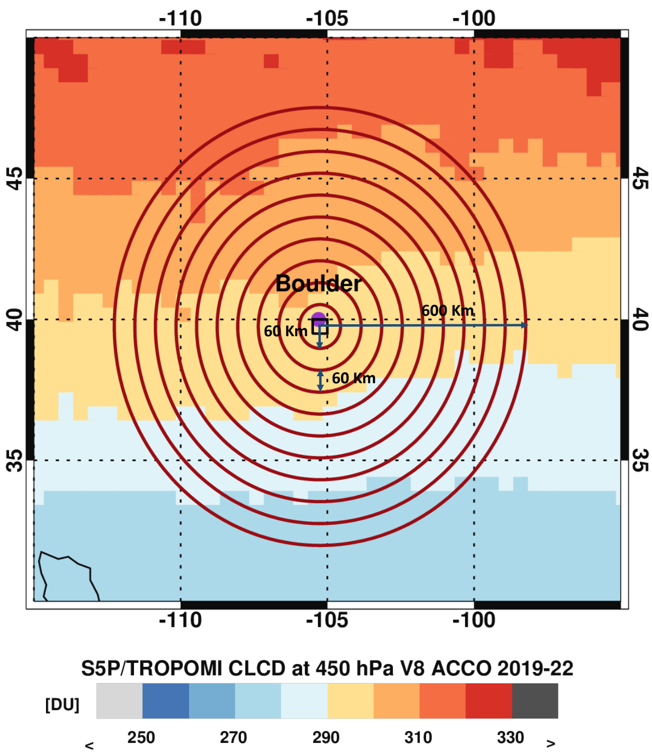

Figure 2. The variable local cloud reference sectors (red circles), ranging from the smallest (60 km) to the largest (600 km), which are centred to the grid box nearest to the Boulder ozonesonde station (40°N, 105.3°W). The smallest sector containing at least 20 cloudy pixels is used to average the ACCO. The background displays a global map of the four-year average TROPOMI ACCO for the period 2019–2022.

4.2 Uncertainty budget

In this section, we establish the uncertainty of CLCD tropospheric ozone. The total uncertainty in daily tropospheric column
175 ozone (u_{TCO}) is estimated using equation 1.

$$u_{TCO} = \sqrt{\frac{u^2_{TOZ_{retrieval}}}{N_{TOZ}} + \frac{u^2_{ACCO_{retrieval}}}{N_{ACCO}} + u^2_{ACCO_{CF}} + u^2_{ACCO_{CTH}} + \overline{u_{TOZ}}^2 + \overline{u_{ACCO}}^2} \tag{1}$$

$u_{TOZ_{retrieval}}$ is the estimated uncertainty for a single total column ozone retrieval ($\approx$ 3 DU), while $u_{ACCO_{retrieval}}$ represents the uncertainty in the ACCO retrieval ($\approx$ 2.5 DU). The uncertainty in the cloud fraction (u_{CF}) is about ± 0.1, contributing less than 1 DU to $u_{ACCO_{CF}}$. The uncertainty associated with cloud-top-height u_{CTH} is $\approx$ 500 m, adding less than 0.5 DU
180 ($u_{ACCO_{CTH}}$) to the TCO measurement uncertainty (Leventidou et al., 2016). The variable N_{TOZ} denotes the number of cloud-free total ozone measurements daily available within each $0.5° \times 0.5°$ grid box for the CLCD method, while N_{ACCO} represents the number of above-cloud column ozone measurements within the cloud reference sector. The terms $\overline{u_{TOZ}}$ and

https://doi.org/10.5194/egusphere-2025-306
Preprint. Discussion started: 17 February 2025

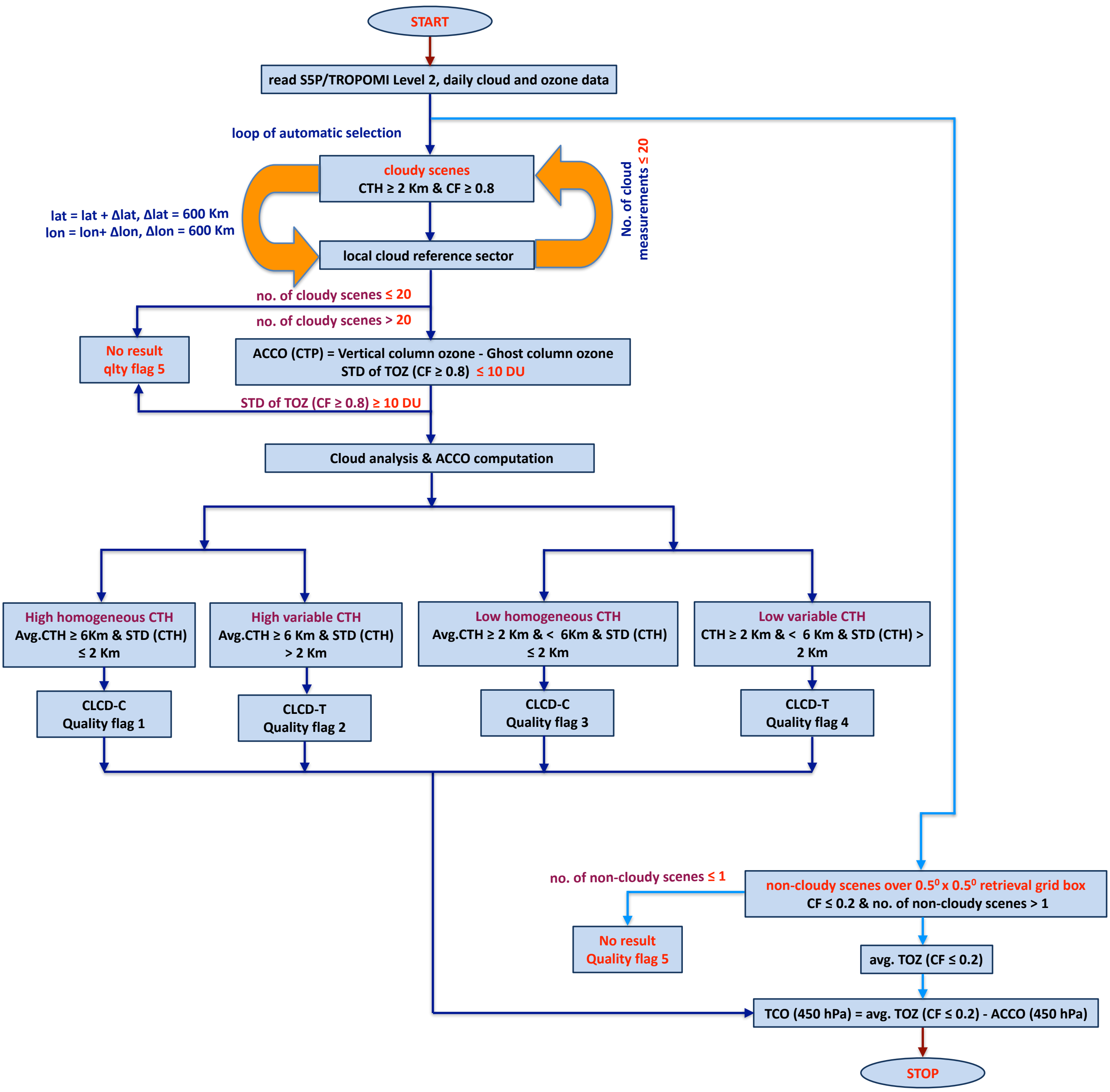

Figure 3. Flow diagram of the CLCD algorithm used for retrieving tropospheric ozone from the surface to 450 hPa level.

$u_{\overline{ACCO}}$ denote the standard deviation (1σ) of the average total ozone under clear sky conditions (CF $\leq$ 0.2) and the ACCO from the local cloud reference sector, respectively (Maratt Satheesan et al., 2024).

https://doi.org/10.5194/egusphere-2025-306
Preprint. Discussion started: 17 February 2025

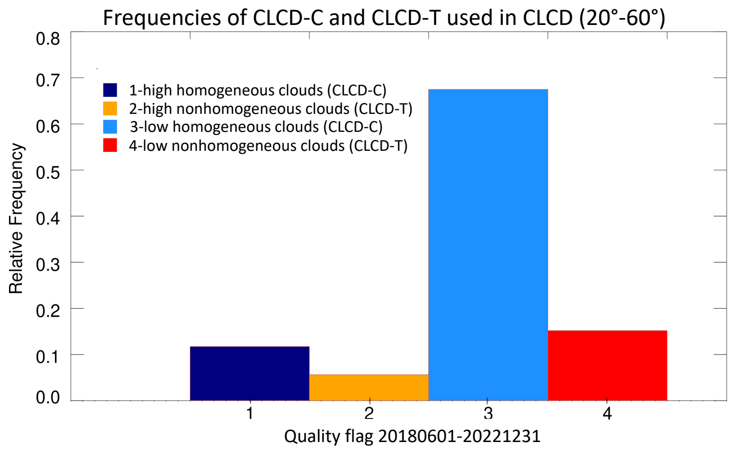

Figure 4. Frequency of the four different CLCD-C and CLCD-T methods applied in CLCD in the extratropics. Distribution for CLCD retrievals based on cloud characteristics for latitudes $\geq 20°$ from 2018 to 2022. Different cloud conditions determine the use of either CLCD-C or CLCD-T (Theil-Sen regression) approach for retrieving ACCO. Quality flags from 1 to 4 are assigned to tropospheric ozone columns based on the range and variability of cloud-top-heights observed in the reference sector. The CLCD-C method is applied when CTH values are homogeneous, with high clouds labelled as quality flag 1 and low clouds as quality flag 3. CLCD-T is used for variable CTH, with high clouds given quality flag 2 and low clouds quality flag 4.

The 5-year average of the daily uncertainties for June and December (2018–2022) is shown in Fig. 5. The average uncertainty in the tropospheric ozone column for both months is approximately 4 DU.

The regions with the highest uncertainty typically have fewer cloudy or clear-sky scenes. The data gaps observed in the figure may result from the filtering criteria and the absence of cloudy or clear sky scenes (Maratt Satheesan et al., 2024). The primary source of uncertainty in the tropospheric ozone column is attributed to the ACCO retrieval and associated cloud parameters (Leventidou et al., 2016).

The uncertainty is significantly higher in June in the Southern Hemisphere (SH) than in the Northern Hemisphere (NH) beyond 40° latitude (Fig. 5a). This increased uncertainty correlates with a rise in the standard deviation of clear-sky total ozone at these latitudes, driven primarily by greater stratospheric ozone variability during austral winter and reduced sampling (Fig. 6a, c). As a consequence of higher stratospheric ozone variability in the winter hemisphere (Weber et al., 2011; Williams et al., 2019), ACCO becomes more variable and the TCO uncertainty increases (Fig. 6).

The TCO uncertainty is also higher in some areas around the middle Atlantic and Pacific data gaps (Fig. 5a, b). The lower sampling rate in these areas contributes to a higher standard deviation of the ACCO measurements (Fig. 6b,d). In June clouds in these regions originate from relatively distant locations and are easily distinguished by their differing cloud-top-heights compared to the surrounding areas (Fig. 6e and f). For example, higher clouds are observed in some areas around the data gaps in the south-central eastern Pacific and the Atlantic (Fig. 6e). This inhomogeneity in cloud-top-height, combined with

https://doi.org/10.5194/egusphere-2025-306
Preprint. Discussion started: 17 February 2025

fewer samples, increases uncertainty in ACCO (Fig 6b). Clear-sky total ozone's relatively low standard deviation contributes to overall lower uncertainties in the same region (Fig. 6a).

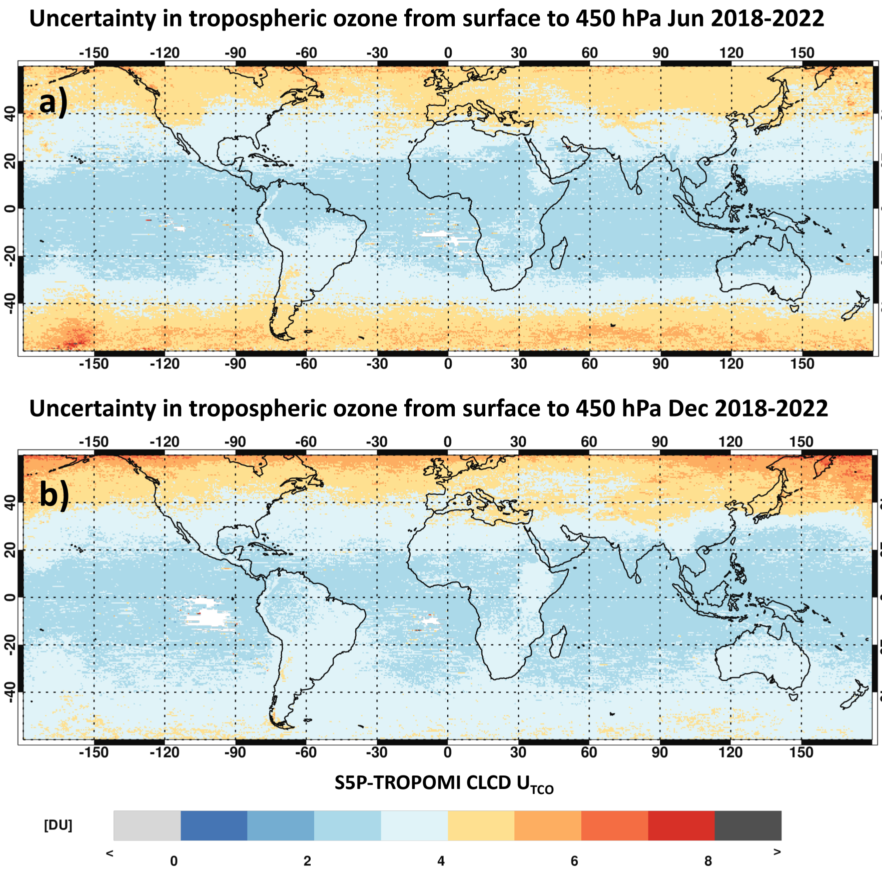

Figure 5. Mean of daily CLCD-TCO uncertainties [DU] from 2018 to 2022 for a) June and b) December.

https://doi.org/10.5194/egusphere-2025-306
Preprint. Discussion started: 17 February 2025

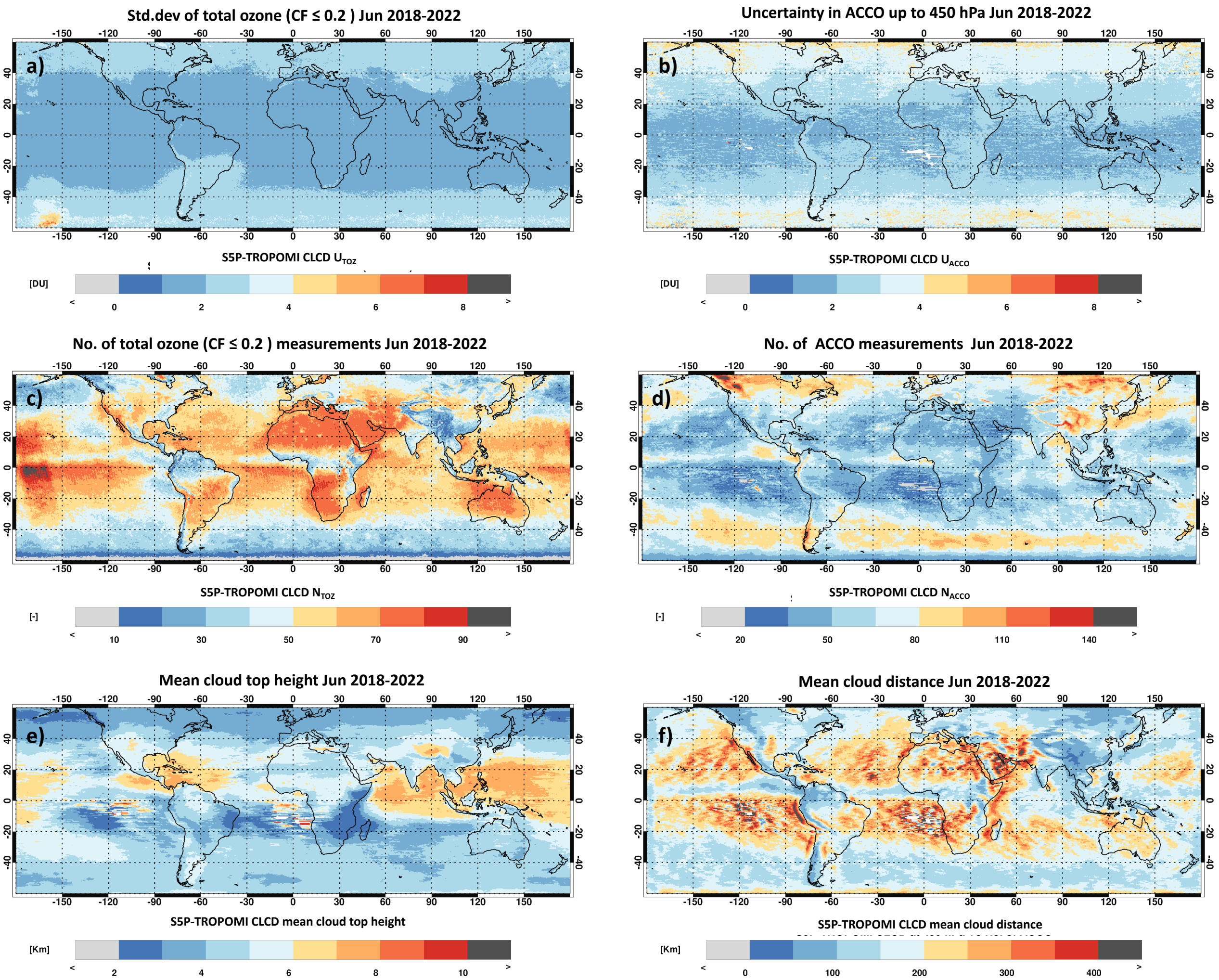

Figure 6. Global maps of (a, b) standard deviation (1σ) of total ozone under clear-sky conditions and ACCO [DU], respectively; (c, d) number of clear-sky total ozone measurements within a $0.5^\circ \times 0.5^\circ$ grid box and ACCO measurements from the reference sector, respectively; (e) average cloud-top-height [km] in the cloud reference sector and (f) average distance [km] of clouds observed by TROPOMI in the reference sector, based on data from 2018 to 2022 for June using the CLCD algorithm.

https://doi.org/10.5194/egusphere-2025-306
Preprint. Discussion started: 17 February 2025

5 Validation and discussions

5.1 Validation by comparisons to ozonesondes

The CLCD TCO results were compared with data from SHADOZ, WOUDC, and NDACC ozonesondes to evaluate the tropospheric ozone accuracy. Monthly mean CLCD tropospheric ozone columns and their corresponding standard deviations (1σ) were computed for the period from June 2018 to December 2022. The locations of the thirty-six ozonesonde stations used for validation are displayed in Fig. 1. The frequency of ozonesonde measurements at these stations ranges from one to fourteen per month, depending on the station.

We compare the monthly averages of the CLCD tropospheric ozone column with those from ozonesonde stations located in the same satellite grid box. Upon reviewing the data, we found that there was a lack of sufficient temporally collocated measurements, particularly at higher latitude stations, for reliable validation. To address this, we decided to compare monthly means of spatially collocated ozonesonde data with CLCD data, ensuring a more robust analysis.

Table 1 lists the mean difference and the 1σ standard deviation of monthly mean tropospheric ozone between CLCD and ozonesondes. The validation results, derived from a diverse set of stations spanning from -54.5°S to 58.7°N, underscore the significant CLCD advantages, particularly in the extratropics and mid-latitude regions.

The differences between CLCD and ozonesonde measurements range from a minimum of -4.0 DU (Hanoi, Vietnam) to a maximum of +5.3 DU (Costa Rica, Central America). Despite these extremes, most of the stations exhibit mean differences within a narrower range of ∼-2 to +2 DU, illustrating that the CLCD method generally provides accurate retrievals with relatively small biases across most regions.

A significant number of stations show minimal biases (close to zero), such as Lindenberg, Germany (0.0 ± 1.9 DU), Payerne, Switzerland (-0.2 ± 1.8 DU), and Uccle, Belgium (0.2 ± 2.2 DU) (Fig. 7). These results imply that the CLCD method performs consistently across mid-latitudes. The standard deviations (spread) range between 1.1 DU and 4.3 DU. Except for Valentia, Ascension and northern most station Churchill, all stations exhibit standard deviations between 1 and 3 DU, indicating moderate variability in the CLCD retrievals. These values highlight the overall reliability of the method.

For instance, standard deviations observed at Uccle, Belgium, and Hohenpeissenberg, Germany, are 2.2 and 2.9 DU, while Lindenberg, Germany, has an even lower standard deviation of 1.9 DU. These moderate standard deviations suggest that the CLCD method performs consistently across different stations and atmospheric conditions. Even in locations with complex meteorological conditions, such as high-altitude regions, the standard deviations remain manageable, showcasing the robustness of the CLCD retrieval algorithm.

The CLCD method also works well in remote, isolated locations. For example, at Ascension Island, the mean difference is -4.2 DU with a standard deviation of 3.7 DU, and at Macquarie Island, Australia, the mean difference is 4.8 DU with a standard deviation of 2.5 DU.

The overall mean difference for stations within 60°S to 60°N, covering both mid-latitudes and tropical regions, is 0.6 ± 2.5 DU. The CLCD method generally provides reliable tropospheric column ozone across a broad latitude range. Additionally, CLCD effectively captures seasonal variations in tropospheric ozone across most stations, especially at higher latitudes (Fig. 7).

https://doi.org/10.5194/egusphere-2025-306
Preprint. Discussion started: 17 February 2025

The dynamic selection of the CLCD algorithm between the CLCD-C and CLCD-T-based cloud characteristics enhances its adaptability to variable clouds, resulting in more reliable ozone measurements across diverse atmospheric conditions. Additionally, a circular reference sector at higher latitudes allows for a more localized cloud sector minimizing the impact from stratospheric ozone variability as best as possible.

Figure 8 shows the variation in bias and scatter between CLCD and ozonesondes as a function of various ozone and cloud parameters. The high standard deviations of these parameters introduce additional uncertainty, making it more difficult to identify clear dependencies. We conclude that no dependencies of the mean bias/scatter in TCO retrievals from total ozone, ACCO, and cloud input parameters are observed.

5.1.1 Causes of bias and variability in CLCD-retrievals

Several factors cause the larger biases and scatter in CLCD-TCO retrievals, as detailed in the following subsections. These include the selection of cloud reference sectors, seasonal meteorology, such as the migration of the ITCZ, the application of climatological corrections, and the occurrence of pollution events. Additionally, significant variability in stratospheric ozone, particularly at higher latitudes, and instrument limitations, such as the limited sensitivity of TROPOMI to surface ozone, also contribute to these discrepancies.

Choice of local cloud reference sector

Using a local cloud reference sector, rather than a fixed large reference area, improves the accuracy of ACCO over the tropics, as shown by Maratt Satheesan et al. (2024). This approach is also very suitable for retrieving tropospheric ozone in the extratropics where spatial stratospheric ozone variability is larger. Good agreement between CLCD retrievals and ozonesonde in the extratropics shown before confirms that the local cloud approach is a major factor in improving the retrieval accuracy (Table 1, Fig. 7). The variable circular local cloud reference sector better minimises the impact of the larger stratospheric ozone variability. There are still some drawbacks to the automatic selection of the cloud reference sector, which is often based solely on cloud data availability. In some cases, this can lead to the selection of quite large cloud reference areas that might miss out on the actual local ozone conditions, ultimately reducing the TCO accuracy (Maratt Satheesan et al., 2024).

Cloud characteristics, such as the number of cloudy scenes, cloud-top-height, and the distance of clouds from the retrieval grid box, are critical in assessing the accuracy of CLCD-TCO. These factors vary significantly with the season and geophysical conditions in different regions.

The CLCD retrievals at stations like Goose Bay, Yarmouth, and Macquarie Island highlight these challenges, particularly due to the presence of remote low-level clouds. The Canadian station, Goose Bay (53.3°N, 60.4°W) has bias and scatter that are among the highest (∼4 DU ± 3 DU).

The largest biases with ozonesondes at Goose Bay (Fig. 9a) are observed in late boreal spring (May) and summer (June and July). This is surprising since Goose Bay, located in the NH, typically experiences ample cloud cover during the summer (see Fig. 12c and 11c). The higher cloud cover should ideally lead to more accurate ACCO and TCO retrievals, but instead, differences are maximum, indicating possible issues with retrieving ACCO (Fig. 9a). Clouds over Goose Bay tend to be lower

https://doi.org/10.5194/egusphere-2025-306
Preprint. Discussion started: 17 February 2025

Table 1. Mean difference (md) and 1σ standard deviation (sdev) [DU] between spatially collocated monthly mean TROPOMI TCO retrievals (CLCD) and ozonesondes during the period from June 2018 to December 2022.

Station	Latitude	Longitude	Data archive	CLCD-TCO md (±) sdev [DU]
Churchill, Canada (CH)	58.7	-94.1	WOUDC-HEGIFTOM	4.6 ± 4.2
Edmonton, Canada (ED)	53.5	-114.1	WOUDC-HEGIFTOM	4.1 ± 3.0
Goose Bay, Canada (GB)	53.3	-60.4	WOUDC-HEGIFTOM	4.4 ± 3.0
Legionowo, Poland (LN)	52.4	21.0	WOUDC-HEGIFTOM	0.3 ± 1.9
Lindenberg, Germany (LB)	52.2	14.1	WOUDC	0.0 ± 1.9
Valentia, Ireland (VA)	51.9	-10.3	WOUDC-HEGIFTOM	1.3 ± 4.3
Uccle, Belgium (UC)	50.9	4.3	WOUDC-HEGIFTOM	0.2 ± 2.2
Port Hardy, Canada (PH)	50.7	-127.4	WOUDC-HEGIFTOM	2.3 ± 3.4
Hohenpeissenberg, Germany (HB)	47.8	11.0	WOUDC-HEGIFTOM	2.5 ± 2.9
Payerne, Switzerland (PY)	46.5	6.6	WOUDC-HEGIFTOM	-0.2 ± 1.8
Yarmouth, Canada (YA)	43.9	-66.1	WOUDC-HEGIFTOM	3.2 ± 2.8
Haute-Provence, France (HP)	43.9	5.7	NDACC-HEGIFTOM	0.3 ± 2.2
L'Aquila, Italy (AQ)	42.3	13.3	WOUDC-HEGIFTOM	-1.5 ± 2.0
Vigne di Valle, Italy (VV)	42.1	12.2	WOUDC-HEGIFTOM	-1.2 ± 2.3
Trinidad Head, California, USA (TD)	40.8	-124.2	WOUDC-HEGIFTOM	0.3 ± 2.9
Madrid, Spain (MA)	40.5	-3.6	WOUDC-HEGIFTOM	0.9 ± 1.8
Boulder, United States (BO)	40.0	-105.3	NDACC-HEGIFTOM	-0.4 ± 1.5
Tsukuba, Japan (TS)	36.1	140.1	WOUDC	-1.1 ± 2.4
Pohang, Korea (PO)	36.0	129.4	WOUDC	-3.1 ± 3.3
Izana, Spain (IZ)	28.3	-16.5	NDACC-HEGIFTOM	-2.7 ± 1.7
King's Park, Hong Kong (KP)	22.3	114.2	WOUDC	-3.9 ± 2.6
Hanoi, Vietnam (HA)	21.0	105.8	SHADOZ-HEGIFTOM	-4.0 ± 2.1
Hilo, United States (HI)	19.4	-155.4	SHADOZ-HEGIFTOM	0.9 ± 1.4
Costa Rica, Central America (CO)	10.0	-84.0	SHADOZ-HEGIFTOM	5.3 ± 1.6
Paramaribo, Surinam (PA)	5.8	-55.2	SHADOZ-HEGIFTOM	2.9 ± 1.2
Kuala Lumpur, Malaysia (KL)	2.7	101.7	SHADOZ-HEGIFTOM	-1.6 ± 1.8
Nairobi, Kenya (NA)	-1.3	36.8	SHADOZ-HEGIFTOM	3.1 ± 1.7
Natal, Brazil (NT)	-5.4	-35.4	SHADOZ-HEGIFTOM	0.4 ± 1.2
Ascension Island, United Kingdom (AS)	-8.0	-14.4	SHADOZ-HEGIFTOM	-4.2 ± 3.7
Pago Pago, American Samoa, (SA)	-14.4	-170.6	SHADOZ-HEGIFTOM	1.1 ± 1.2
Suva, Fiji (FI)	-18.1	178.4	SHADOZ-HEGIFTOM	-0.5 ± 1.7
Reunion, France (RE)	-21.1	55.5	SHADOZ-HEGIFTOM	0.3 ± 1.1
Irene, South Africa (IR)	-25.9	28.2	SHADOZ-HEGIFTOM	0.0 ± 1.5
Broad meadows, Australia (BM)	-37.7	144.9	WOUDC	1.5 ± 1.9
Lauder, New Zealand (LA)	-45.0	169.7	WOUDC-HEGIFTOM	1.3 ± 1.7
Macquarie Island, Australia (MI)	-54.5	158.9	WOUDC	4.8 ± 2.5
overall (60°S−60°N)				0.6 ± 2.5

https://doi.org/10.5194/egusphere-2025-306
Preprint. Discussion started: 17 February 2025

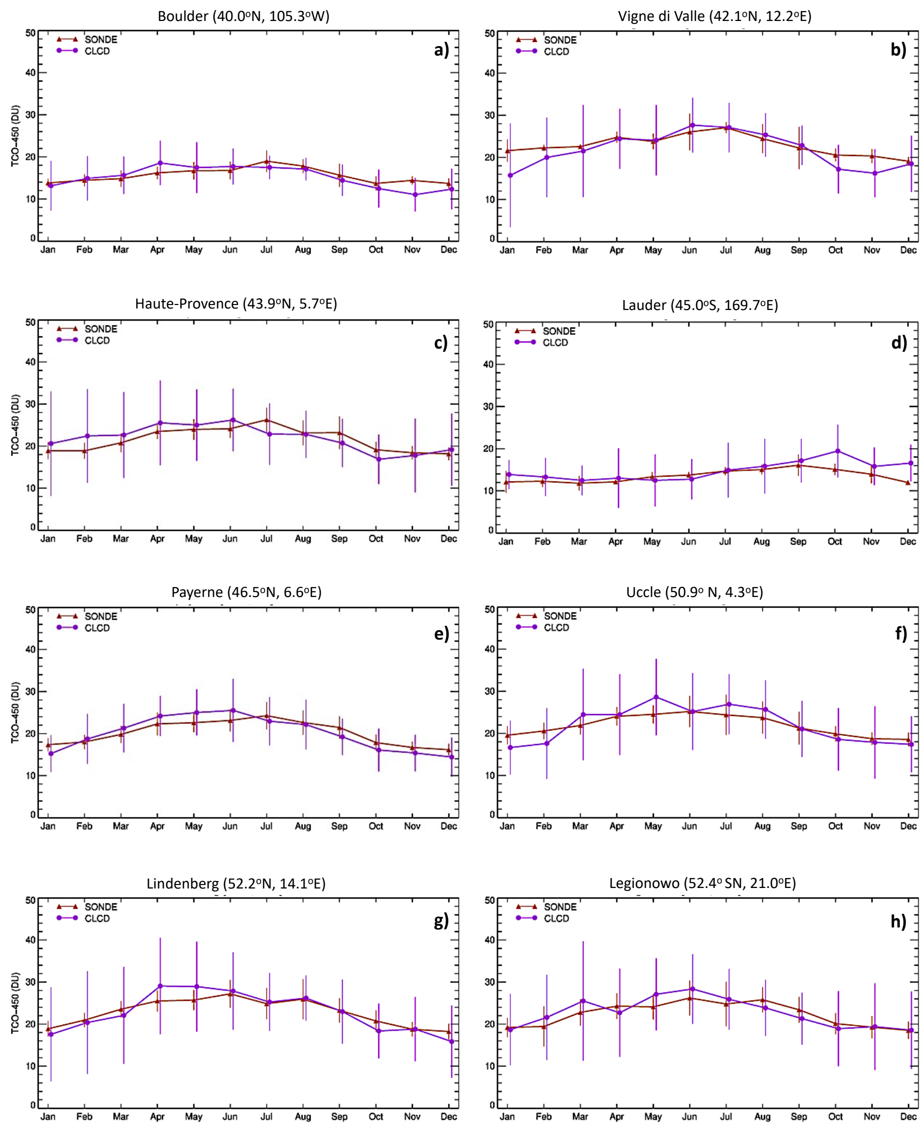

Figure 7. Seasonal variation of TROPOMI and ozonesonde tropospheric ozone columns above 450 hPa at selected ozonesonde sites (40°-55°) for the period between July 2018 and December 2022. The brown and blue lines are TROPOMI and sondes, respectively. The error bars are the standard deviations (1σ) from taking the monthly mean. No error bars are shown for stations with only one launch per month. The stations selected here have small biases of CLCD to sondes (see Table 1).

https://doi.org/10.5194/egusphere-2025-306
Preprint. Discussion started: 17 February 2025

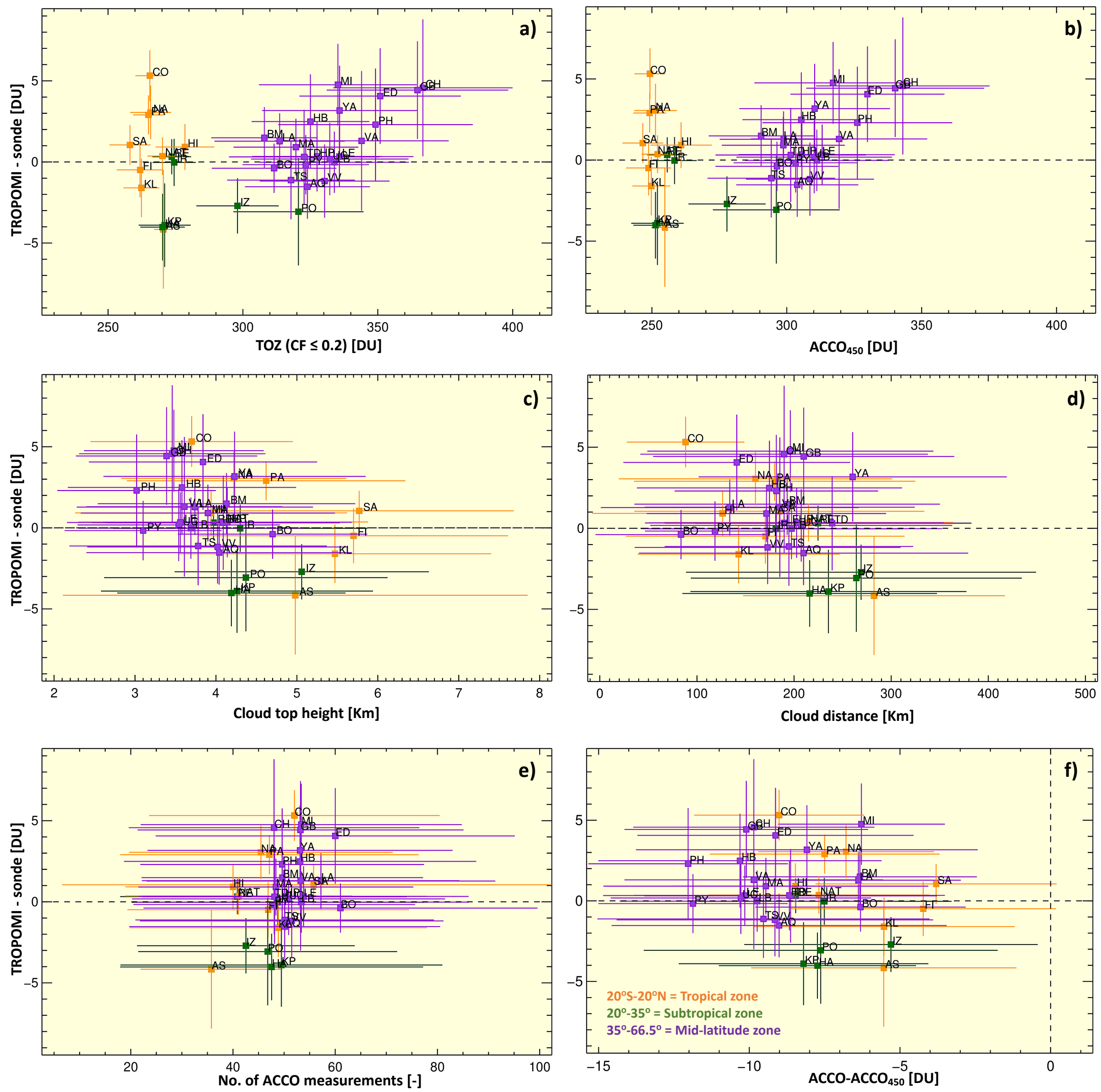

Figure 8. Scatter plot of mean differences (md, TROPOMI – sonde) with 1σ standard deviation [DU] and the respective average a) total ozone under clear sky conditions (CF $\leq$0.2) [DU], b) ACCO up to 450 hPa (CF $\geq$0.8) [DU], c) cloud-top-height [km], d) mean distance of clouds [km], e) the number of ACCO measurements from the reference sector, and f) the difference between actual ACCO and ACCO below 450 hPa level [DU] during the time period from 2018 to 2022. The different colours of the symbols represent stations from different zonal bands.

https://doi.org/10.5194/egusphere-2025-306
Preprint. Discussion started: 17 February 2025

in altitude and are from more distant locations (Fig. 8c and d). The presence of remote low-level homogeneous clouds during boreal spring months (Fig. 11b and 12b) favours the CLCD-C method for ACCO retrieval over the CLCD-T. This results in larger differences between the mean cloud-top-pressures and the reference level of 450 hPa, thus requiring a significant climatological correction on the order of -10 DU to adjust ACCO to 450 hPa (Fig 8f). This excessive climatological correction may lead to lower ACCOs (Fig. 8b) and higher tropospheric ozone columns (Fig. 9a).

Moreover, local pollution events, including summer ozone enhancements from North American wildfires over Goose Bay, as noted by Moeini et al. (2020), may be missed in ACCO retrievals due to the influence of distant clouds (Fig. 11c). However, these events could still reflect in total ozone (TOZ) retrievals (Fig. 8a), leading to a significant positive bias in TCO estimation.

Similarly, Yarmouth has persistent rather remote clouds throughout the year, regardless of the season (Fig. 11), which poses a significant challenge for retrieving ACCO. The difference between observed ACCO and the ACCO up to 450 hPa is notably larger at this site (Fig. 8f). This may lead to larger adjustments to the reference level, potentially causing TCO to be too high, especially during late boreal winter and early spring (Fig. 9b). In summary, the high positive bias in TCO is most likely caused by low-level remote clouds.

At the southernmost station, Macquarie Island (54.5°S, 158.9°E), CLCD retrievals exhibit the second-highest bias and variability among all stations (4.8 ± 2.5 DU). This is expected due to the higher stratospheric ozone variability commonly observed at higher latitudes (Williams et al., 2019; Cooper et al., 2014). The cloud conditions are similar to the NH stations Goose Bay and Yarmouth. The impact of pollution events, however, does not play a role here given its isolation from the Australian mainland and location in the remote Southern Ocean, far from potential local pollution sources (Greenslade et al., 2017).

According to Greenslade et al. (2017), Macquarie Island experiences stratosphere-troposphere transport events primarily during boreal autumn and early winter months. These events likely led to the transport of stratospheric ozone into the upper troposphere, which should have been detected as Above Cloud Column Ozone and contributed to an actual ACCO enhancement during these periods. However, the presence of remote clouds in autumn and winter (Fig. 11d and a) may have missed this actual ozone abundance, resulting in an underestimation of ACCO (Fig. 8b) and a subsequent overestimation of TCO during these months. The seasonal variability (Fig. 9h) supports this interpretation, showing the largest differences between the CLCD-TCO retrievals and ozonesonde data during the autumn and winter months.

Biases can also arise when clouds are scarce within the local reference sector. Limited cloud coverage reduces the available ACCO data, increasing scatter in the final TCO estimates. Ascension Island (8°S, 14.4°W) exemplifies this issue as it has the fewest ACCO measurements of all stations (Fig. 8e and 9g) even after using the largest cloud reference sectors (Fig. 8d). The station also exhibits the highest cloud-top-height variability, ranging from a minimum of ∼2 Km to 8 Km (Fig. 8c). This variability necessitates corrections or differences added to ACCO, spanning ∼-10 DU to -1 DU. The limited data and high variability in cloud-top-heights could explain the relatively higher standard deviation (∼4 DU) observed over Ascension (Table 1 and Fig. 9g).

Seasonal shift of ITCZ

The seasonal migration of the Intertropical Convergence Zone (ITCZ) significantly influences the accuracy of TCO retrievals, particularly at locations like King's Park (22.3°N, 114.2°E), exhibiting the highest negative bias of ∼4 DU (Table 1). During boreal autumn and winter, the ITCZ shifts southwards and across the equator, resulting in fewer cloudy scenes available for ACCO retrievals in this region. As the ITCZ moves away, the frequency of remote low-level clouds over this subtropical station increases during boreal autumn and winter (Fig. 12d, a and Fig. 11d, a). The larger cloud reference sectors with low-level clouds lead to overestimated ACCOs, which cause a negative bias in TCO as illustrated in Fig. 9d.

In King's Park, CLCD generally shows lower tropospheric ozone columns than ozonesondes in all seasons, except in June. During early boreal summer, CLCD-TCO agree well with ozonesondes, likely due to the presence of higher cloud-top-heights due to the ITCZ near the station (Fig. 12c and Fig. 11c).

Climatological corrections

The CLCD-C method in the CLCD algorithm may introduce additional uncertainties due to the climatological corrections applied when ACCO is converted to the 450 hPa reference level. This is especially true in regions with prevalent low-level clouds, where a longitudinally invariant climatology may fail to replace the actual local atmospheric variations. For instance, stations like Costa Rica show both the highest positive bias and the largest correction applied to adjust ACCO to the reference level (∼ -9 DU) among tropical stations (Fig. 8f).

Nonetheless, despite applying the largest correction to the 450 hPa level (∼-9 DU), Payerne remains one of the stations with the best CLCD-TCO agreement with ozonesonde data (Fig. 7e). Similarly, other mid-latitude stations show substantial corrections yet maintain good agreement with ozonesonde (Fig. 7). Hence the overall analysis of Fig. 8 indicates no significant dependence between the correction to the reference level and the mean bias and scatter in CLCD retrievals. This indicates that large corrections to the reference altitude are not a general predictor of bias.

However, it's possible that these corrections may not perform well at certain stations. While climatological adjustments are generally designed to provide an average or "typical" correction for ozone columns, they may not capture the unique or highly variable atmospheric conditions at some stations. This is especially true for regions where ozone distribution is influenced by local or seasonal phenomena, such as Costa Rica, which is located near the ITCZ, experience significant seasonal shifts in cloud cover and vertical mixing that climatological averages may not adequately represent.

Upon closer examination of Fig. 11, it is obvious that the clouds used for ACCO retrievals at this site are generally located nearby, except during boreal winter and spring seasons (Fig. 11a). This shift is attributed to the southward migration of the ITCZ, as discussed in the previous subsection. Additionally, the cloud-top-heights over Costa Rica are relatively low and homogeneous, particularly during boreal winter and spring, as depicted in Fig. 8c and Fig. 12a and b.

These lower homogeneous cloud tops favour the CLCD-C approach over CLCD-T and necessitate larger climatological corrections to adjust the ACCO retrievals to the reference altitude of 450 hPa (Fig. 8f). This results in a negative bias in ACCO up to 450 hPa level (Fig. 10a and b) and a positive bias of the tropospheric column ozone in winter and spring (Fig. 9f).

https://doi.org/10.5194/egusphere-2025-306
Preprint. Discussion started: 17 February 2025

The CLCD-T method in CLCD offers a key advantage by directly determining the mean ACCO, thereby avoiding the need for climatological corrections. This method requires a sufficiently high number of ACCOs in the reference sector. To address this, a minimum of twenty ACCO measurements from the cloud reference sector is required when retrieving TCO to ensure accuracy. Even though the Theil-Sen regression handles outliers well, they still impact the TCO accuracy. This impact is reduced by using the homogeneity criteria for the total ozone under cloudy conditions. The CLCD-C is applied more frequently than CLCD-T in the extratropics (Fig. 4).

Influence of biomass burning/stratospheric ozone streamers

Although retrieving ACCO from local clouds makes TCO more reliable, there are certain drawbacks. One issue occurs when stratospheric ozone streamers or pollution events from biomass burning near or within the retrieval grid box influence the assessment of stratospheric ozone. This can result in an overestimation of ACCO and an underestimation of CLCD-TCO, even though the homogeneity criteria help mitigate this issue to a certain extent. Two stations, Hanoi (21°N, 105.8°E) in Southeast Asia and Ascension Island (8°S, 14.4°W) in the Atlantic Ocean, exemplify such scenarios. Both stations exhibit the largest negative biases in TCO retrievals, approximately ∼-4 DU.

Over Hanoi, the CLCD method consistently underestimates TCO throughout the year, with the largest discrepancies occurring in early spring and September (Fig. 9e). The exchange between the tropical troposphere and the extratropical stratosphere enhances ozone concentrations in this region. Previous studies have observed increasing tropospheric ozone during boreal spring, partly driven by biomass burning in nearby regions such as Thailand (Liao et al., 2021; Sonkaew and Macatangay, 2015; Ogino et al., 2022), and possibly due to lower stratosphere-upper troposphere transport linked to the subtropical jet passing over Hanoi (Yonemura et al., 2002). This transport process also likely contributes to higher tropospheric ozone columns in early autumn (Fig. 9e). It is probable that ACCO retrievals over nearby clouds during spring and autumn (Fig. 11c, d) are influenced by these tropospheric ozone increases, leading to higher ACCO values and, in turn, lower tropospheric ozone compared to sondes.

Similarly, Ascension Island, located in the Atlantic Ocean, is affected by pollution from biomass burning in central and southern Africa. Ground-based observations over Ascension reveal peak ozone concentrations from July to October, with an additional spike in February likely tied to biomass burning in western and northern Africa (Fishman et al., 1992; Jensen et al., 2012). Conversely, the lowest TROPOMI TCO levels occur in mid-spring (April), corresponding with the northward movement of the ITCZ (Fig. 9g).

CLCD-TCO retrievals over Ascension show the least agreement with ozonesondes during late boreal summer and early autumn when low-level clouds over the island dominate. These clouds likely contribute to a high bias in ACCO and a low bias in TCO. Biomass burning in southern Africa and South America peaks during late boreal winter and autumn (Wai et al., 2014), which may introduce positive biases in ACCO measurements (Fig. 10c, d and Fig. 8b) and negative biases in TCO by CLCD. The observed high scatter and biases in the CLCD retrievals at Ascension can likely be attributed to the limited number of available measurements, the retrievals over clouds from different latitudes, the variability in cloud cover, and the influence of biomass burning.

https://doi.org/10.5194/egusphere-2025-306
Preprint. Discussion started: 17 February 2025

Stratospheric ozone variability at higher latitudes

At higher latitudes, where stratospheric ozone variability is greater, the CLCD method may struggle to provide accurate retrievals. The complex stratospheric ozone dynamics can further complicate the retrievals despite the homogeneity criteria applied.

Total ozone peaks at higher latitudes during winter/spring due to the increased ozone transport from the tropical source region. This transport process is notably weaker during summer and early fall and is less pronounced in the SH (Fahey and Hegglin, 2010; Weber et al., 2011) (Fig. 10). This might explain the high spread during spring in almost all the high latitude NH stations, Goose Bay, Yarmouth and Valentia, compared to the SH station Macquarie island (Fig. 9 and Table 1).

The station with the highest observed scatter (±4.3 DU) in tropospheric ozone is Valentia, Ireland (51.9°S, 10.3°W). Analysis of the seasonal variability shows a consistently large spread throughout the year, particularly from February to July (Fig. 9c). This persistent scatter is consistent across different seasons, indicating substantial variability in stratospheric ozone. Valentia exhibits relatively high variability in total ozone under clear sky conditions (Fig. 8a) and in ACCO up to 450 hPa (Fig. 8b and Fig. 10).

The subtropical site King's Park displays a seasonal ozone cycle with a significant peak in boreal spring, as revealed by a 20-year ozonesonde analysis by Liao et al. (2021) (Fig. 9d). This suggests substantial ozone transport from mid-latitude regions, with elevated levels resulting from stratospheric intrusions and biomass burning, which accounts for the large standard deviations in ozonesonde measurements. In contrast, CLCD struggles to capture these complex ozone patterns at King's Park, leading to less agreement with the ozonesonde data.

Limited sensitivity of TROPOMI to surface ozone

The TROPOMI instrument has less than 50% sensitivity to ozone below approximately 700 hPa (∼3 km) (Hubert et al., 2021). This reduced sensitivity can cause ozone from surface pollution events to be underestimated in clear-sky ozone columns, lowering the retrieved CLCD-TCO.

A notable example of this limitation is the ozonesonde station in Hanoi. The city's rapid urbanisation and industrialisation have significantly increased emissions of ozone precursors, leading to higher tropospheric ozone levels (Dam et al., 2008). However, due to TROPOMI's reduced sensitivity to lower atmospheric layers, such elevated surface ozone levels may not be fully detected, further contributing to underestimations in the retrieved ozone columns (see Table 1) (Heue et al., 2022; Sofieva et al., 2022).

In summary, a comprehensive analysis of TCO retrievals across all thirty-six stations and comparisons with ozonesondes suggest that TCO retrievals over stations experiencing complex ozone and cloud dynamics will likely exhibit higher biases.

5.2 Seasonal ozone and cloud variation

The ozone and cloud input data used in the CLCD-TCO retrievals exhibit significant seasonal fluctuations, and understanding these variations is crucial for accurately interpreting their impact on the final tropospheric ozone estimates. Stratospheric

https://doi.org/10.5194/egusphere-2025-306
Preprint. Discussion started: 17 February 2025

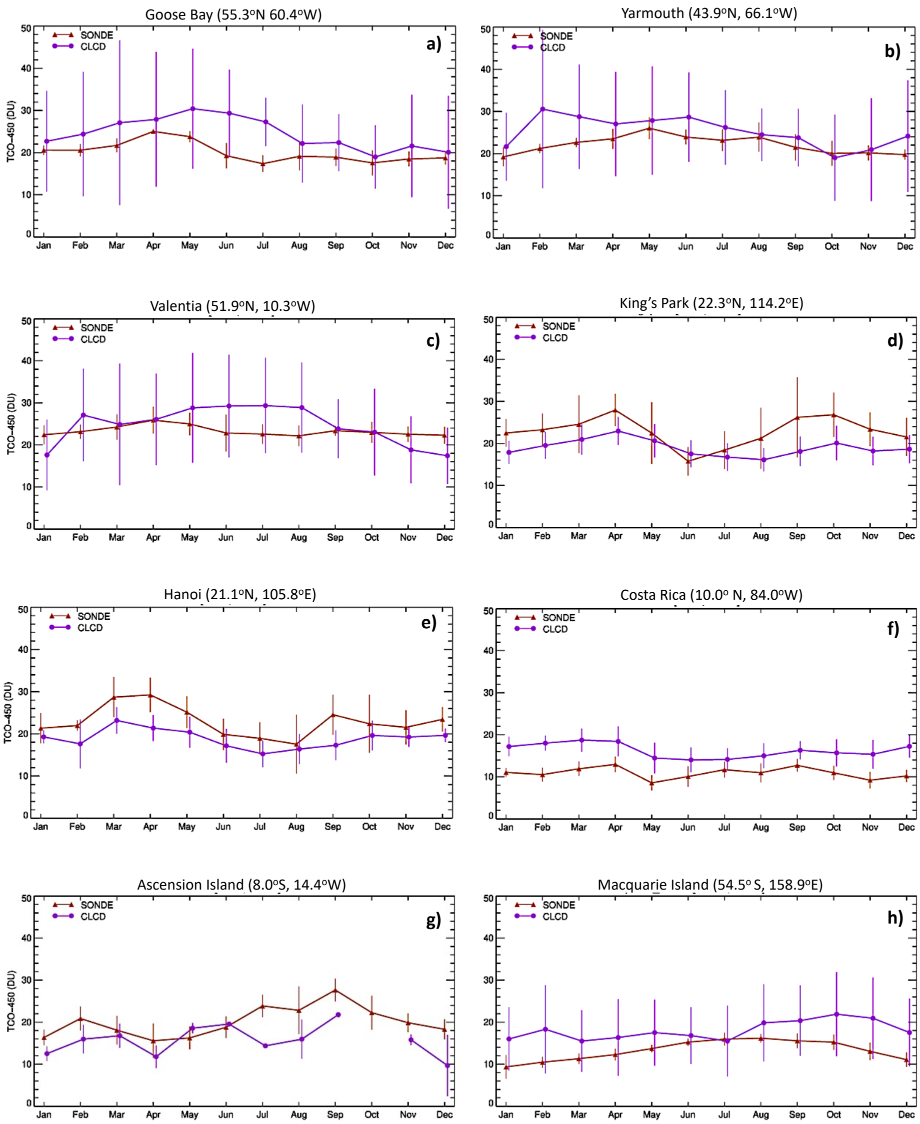

Figure 9. Same as Fig. 7 but the stations selected here have the large biases of CLCD to sondes (see Table 1).

ozone levels and cloud parameters, including cloud-top-height and the distance of clouds from the retrieval grid box, often exhibit significant seasonal shifts. To better capture these patterns, we created whisker plots for ACCO, cloud-top-height, and cloud distance for all four seasons. These plots help us to understand the extent of seasonal variability and its influence on tropospheric ozone retrievals.

https://doi.org/10.5194/egusphere-2025-306
Preprint. Discussion started: 17 February 2025

As shown in Figure 10, the winter hemispheric stations (especially those in extratropical regions) exhibit greater stratospheric variability (Weber et al., 2011; Williams et al., 2019). This variability is particularly pronounced for stations beyond 35° latitude.

Figure 11 illustrates the seasonal variability in the mean distance of clouds used for ACCO calculations across all stations. The analysis reveals no significant relationship between cloud distance and latitude during any of the four seasons.

The tropical station at Ascension Island consistently shows remote cloud distances across seasons, except boreal autumn (Fig. 11d). In contrast, Costa Rica tends to have nearby clouds because of its proximity to the equator, resulting in shorter cloud distances for ACCO retrievals over this station. Cloud distance variability is influenced by station-specific factors such as location, local geography, and regional climate. For example, the mid-latitude station Pohang consistently experiences remote clouds throughout the years independent of seasons.

Some NH tropical and subtropical stations, like Costa Rica, Hanoi, and King's Park, exhibit low-level clouds during the boreal winter and relatively higher cloud-top-heights in the summer (Fig. 12). Similarly, the SH subtropical station Reunion shows a seasonal pattern with higher average cloud-top-heights during the austral summer and autumn.

Stations in the Pacific sector (Hilo, Fiji, Samoa, and Kuala Lumpur) generally have high cloud-top-heights, regardless of the season (Ziemke et al., 1998; Leventidou et al., 2016; Hubert et al., 2021; Maratt Satheesan et al., 2024). Among these, Fiji and Samoa experience the highest cloud-top-heights in all seasons. Mid-latitude stations tend to show less seasonal variability and generally have lower cloud-top-heights than tropical stations (Fig. 4). Payerne, a mid-latitude station, consistently experiences the lowest cloud-top-heights in nearly all seasons.

5.3 Meridional variation of statistical bias and dispersion

From Fig. 13, it is evident that the CLCD algorithm overestimates TCO retrievals across most stations. Twenty-two of thirty-six global stations display positive mean differences. In the tropics, the CLCT algorithm tends to outperform CLCD, except at Kuala Lumpur (2.7°N, 101.7°E).

The CLCD algorithm performs better than CLCT in the subtropics (20°- 35°), where it benefits from a circular cloud reference sector with more cloudy pixels being more representative of local cloud conditions in the grid-box. The comparatively large bias and standard deviations observed with the CLCT algorithm are expected, given the complex ozone dynamics in the subtropics compared to the tropics. Due to high variability in the ACCO measurements, the CLCT approach tends to underestimate the tropospheric ozone column at all subtropical stations except Reunion, similar to TCO retrievals at 270 hPa (Maratt Satheesan et al., 2024).

Within the latitude range of 20° to 45 °, the mean differences are more varied compared to higher latitudes (≥45°). Both positive and negative biases are observed. Standard deviations are generally lower in this range than at higher latitudes. At higher latitudes, there is a tendency for positive biases in the TROPOMI TCO. The mean differences range from -0.2 DU to 4.8 DU, with larger standard deviations (∼2-4 DU), reflecting greater variability in this region (Fig. 13).

In summary, CLCD-TCO retrievals at higher latitudes tend to exhibit positive biases with higher variability (overall average standard deviation of ∼3 DU), while retrievals below 45° (20°-45°) show both positive and negative biases, with lower spreads

https://doi.org/10.5194/egusphere-2025-306
Preprint. Discussion started: 17 February 2025

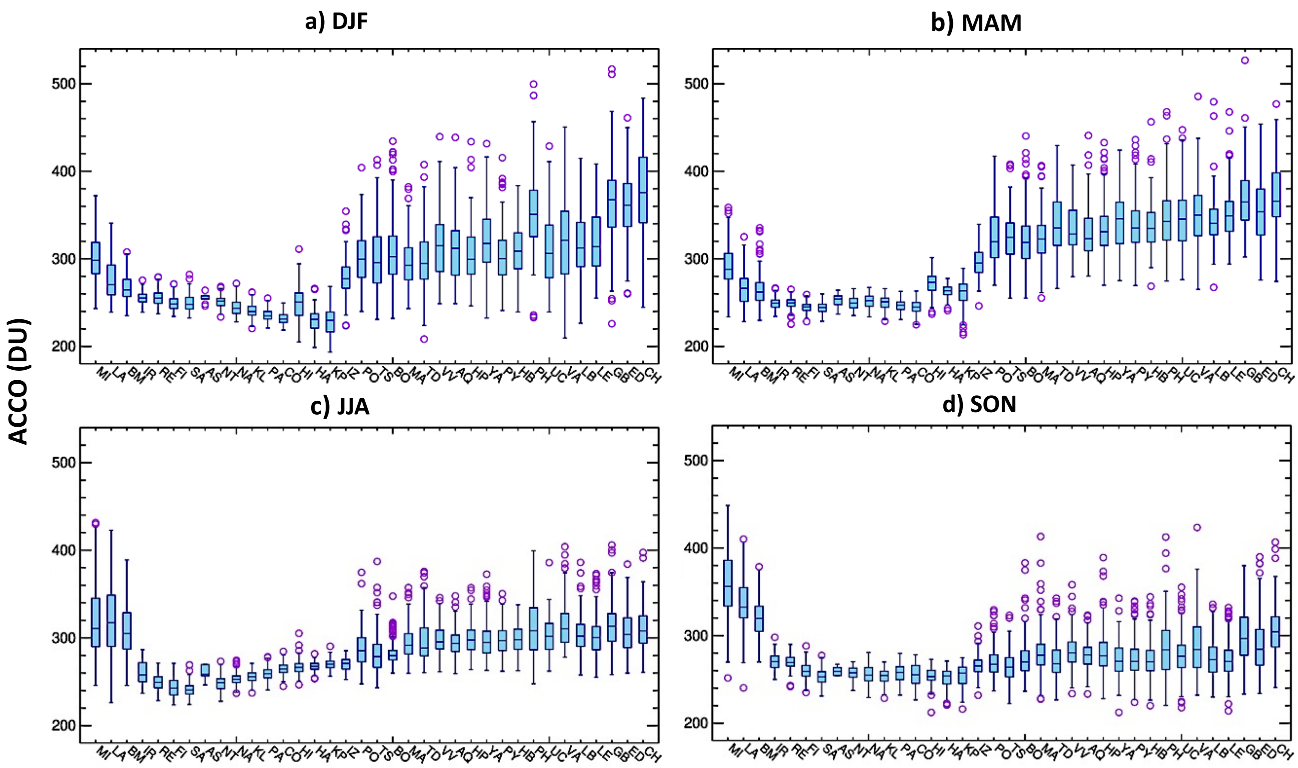

Figure 10. Seasonal mean above cloud column ozone [DU] from CLCD for each ozonesonde station in the time period from June 2018 to December 2022. The stations are ordered from left to right with increasing latitude. Seasons are defined as DJF (December, January, February), MAM (March, April, May), JJA (June, July, August), and SON (September, October, November). The lines (whiskers) extending from the box indicate the variability outside the upper (75th) and lower (25th) quartile. The horizontal line on the box represents the median or 50th percentile. The dark magenta circles represent outliers. Abbreviations for stations can be found in Table 1.

(∼2 DU). In the tropics (20°S - 20°N), the average scatter remains nearly the same (∼2 DU), with most stations showing positive biases.

The NH exhibits a broader range of biases, from ∼-4.0 DU to ∼5.3 DU, reflecting more varying atmospheric conditions, ozone dynamics, and cloud cover patterns. The standard deviations of the biases are moderate to high, ranging from ±1.2 DU to ±4.3 DU. This larger spread in TCO in the NH can be attributed to stronger variability in stratospheric ozone (Fig. 10) (Williams et al., 2019; Cooper et al., 2014).

The SH shows a spread of biases, mostly between -0.5 DU and +4.8 DU (excluding Ascension Island), with all stations exhibiting standard deviations of below 2.5 DU. This overall pattern of lower dispersion in the SH suggests more stable and consistent TCO retrievals, likely due to the lower stratospheric ozone variability and lower regional pollution than in the NH.

https://doi.org/10.5194/egusphere-2025-306
Preprint. Discussion started: 17 February 2025

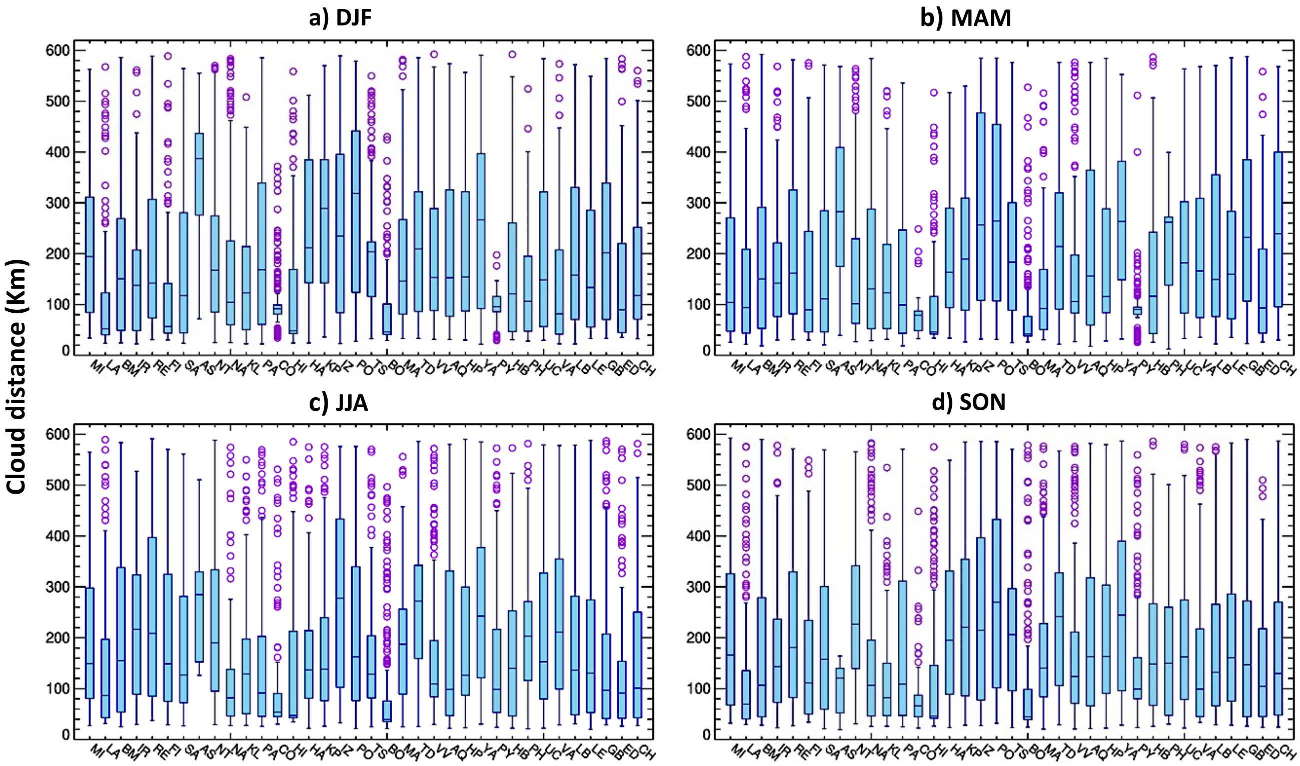

Figure 11. Same as Fig. 10 but for mean distance of cloudy pixels [km] used in the ACCO calculations for the grid box around the ozonesonde station.

5.4 Comparison of CLCD and CLCT in the tropics and subtropics

The CLCT algorithm, the predecessor of the CLCD algorithm, was specifically developed for tropical applications (Maratt Satheesan et al., 2024). In this section, we compare the performance of the CLCT and the new CLCD algorithm in retrieving tropospheric ozone columns up to 450 hPa over the tropics and subtropics.

The CLCD retrievals over the Pacific Ocean sites (70°E-170°W) Fiji, Samoa, Kuala Lumpur, and Hilo show good agreement with ozonesonde measurements, with both bias and scatter remaining within 2 DU (Fig. 14 and 13). Notably, CLCD reduces the bias at Kuala Lumpur from -2.8 DU (CLCT) to -1.6 DU by using a circular reference sector that captures local high-altitude clouds more effectively (Fig. 8c, d).

In general, the tropospheric ozone seasonality over the Pacific Ocean is less pronounced compared to the Atlantic, with variations of ±5 DU (Newton et al., 2016). Additionally, the abundance of clouds and the relatively less polluted background in the Pacific region (Newton et al., 2016) benefit CLCD retrievals, reducing bias and scatter at Pacific sites. However, a noticeable difference exists in the tropospheric ozone patterns over the Southwestern Pacific between CLCD and CLCT (Fig. 14).

https://doi.org/10.5194/egusphere-2025-306
Preprint. Discussion started: 17 February 2025

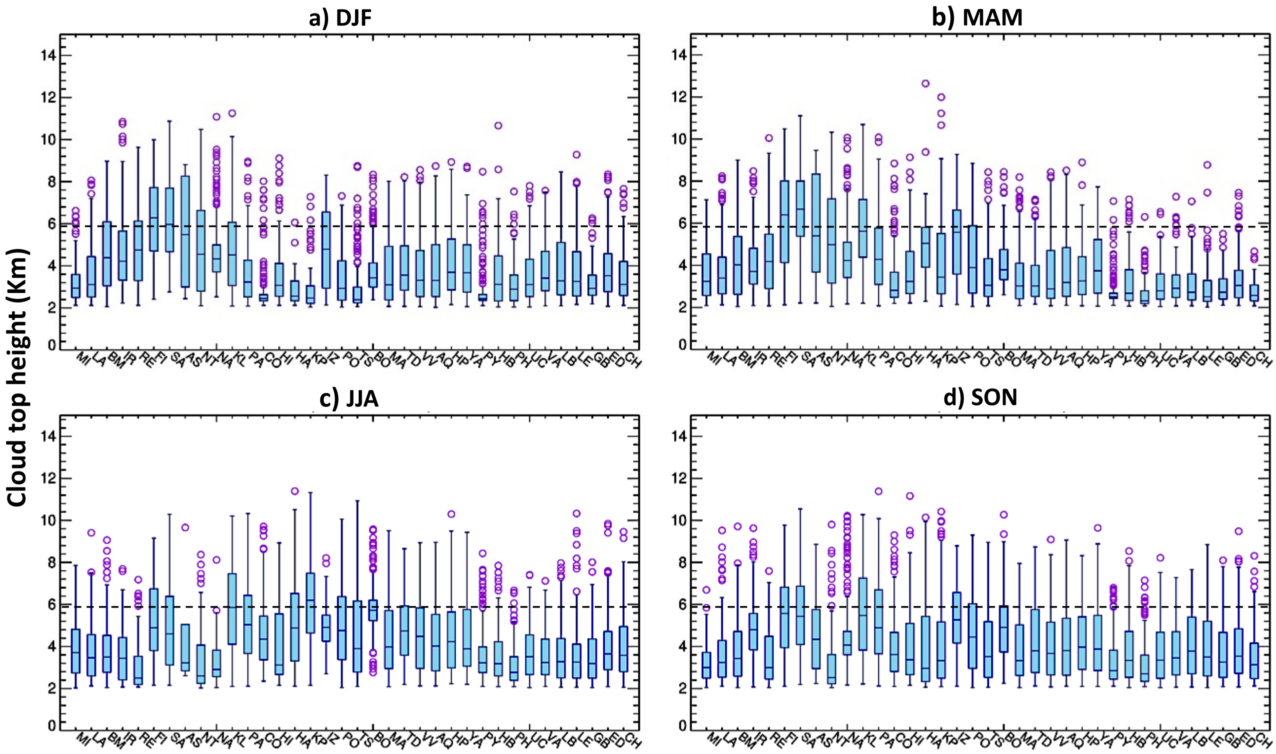

Figure 12. Same as Fig. 10 but for mean cloud-top-height [km] from TROPOMI used in the above cloud column calculation for the grid box around the ozonesonde station. The dashed line represents the 450 hPa level (≈ 5.5km).

In the non-Pacific sector (70°E–170°W), the TCO from the CLCD algorithm is consistently higher than those from CLCT across all sites in the Atlantic basin (except Natal). Over Costa Rica and Paramaribo, CLCD exhibits higher positive biases (5.3 DU and 2.9 DU, respectively), while Ascension Island shows a significant negative bias (-4.2 DU) (see Table 1 and Fig. 13).

The main difference between the two algorithms is the selection of local cloud reference sectors (circular versus longitudinal extension) and using an ozone climatology. CLCD uses a circular reference sector, including nearby clouds from both longitudinal and meridional directions.

Over the South Atlantic station Ascension Island, the CLCD algorithm shows a negative bias of -4.2±3.7 DU. The South Atlantic Ocean is characterised by tropospheric ozone levels reaching up to 40 DU. As discussed in section 5.1.1, the significant scatter and biases in CLCD retrievals at Ascension Island can be mainly linked to the chosen cloud reference sectors. This approach has resulted in fewer ACCO measurements (Fig. 8e) and ACCO retrievals over nearby clouds from different latitudes

https://doi.org/10.5194/egusphere-2025-306
Preprint. Discussion started: 17 February 2025

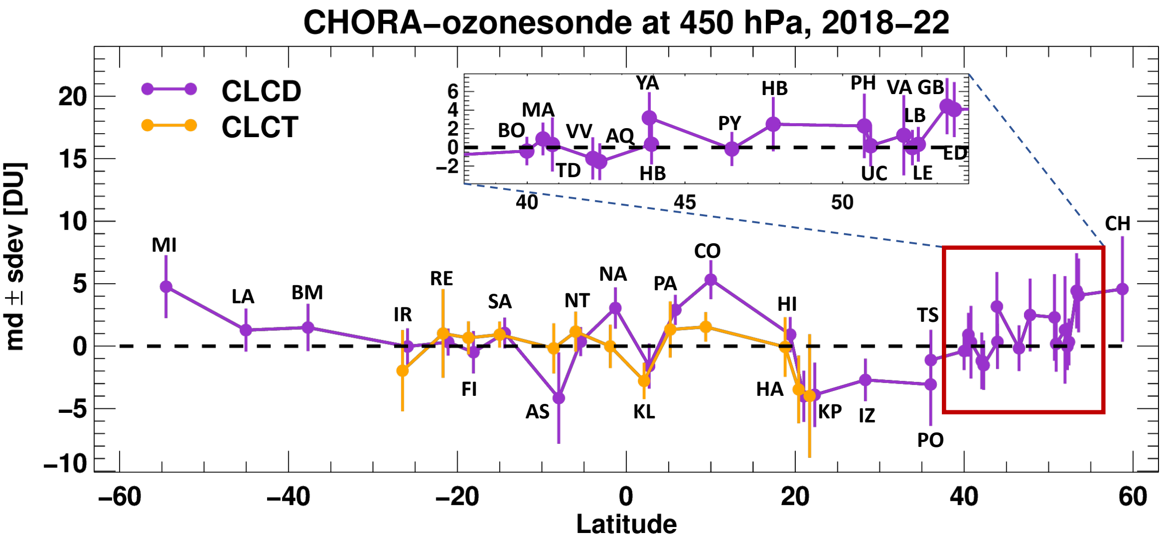

Figure 13. Latitudinal variation of the mean difference (md) and 1σ standard deviation (sdev) [DU] of TROPOMI TCO retrieved using CLCT (yellow) and CLCD (magenta) with respect to HEGIFTOM SHADOZ/WOUDC/NDACC ozonesondes averaged over the period from June 2018 to December 2022.

(Fig. 11), compared to CLCT (see Fig. 12 from Maratt Satheesan et al. (2024)). Using a circular cloud reference sector often selects clouds from different latitudes, introducing air masses that are less representative of the local cloud conditions. This approach might increase the variability in stratospheric ozone, more strongly violating the assumption of its low variability in the tropics a prerequisite for the CCD retrieval. Furthermore, using a small circular cloud reference sector often leads to a higher reliance on ozone climatology, particularly in the tropics, where Theil-Sen regression in CLCT has been shown to provide more reliable ACCO estimation (Maratt Satheesan et al., 2024).

This may explain the absence of high tropospheric ozone concentrations in the South Atlantic in the four-year average CLCD TCO global map (Fig. 14b).

The CLCT algorithm shows a much smaller bias of -0.3±1.9 DU over Ascension Island compared to CLCD. Even when remote clouds are selected (Fig. 12 from Maratt Satheesan et al. (2024)) in CLCT, the east-west moving cloud reference sector helps mitigate inhomogeneities in the stratospheric ozone column. A latitudinally confined but longitudinally varying local cloud reference sector is more suited for the mean ACCO calculation in the tropics. This approach includes more cloud measurements compared to CLCD and effectively fulfils more closely the zonal invariance of stratospheric ozone (Ziemke et al., 1998).

Additionally, the stability of cloud properties, such as cloud-top height and distribution, along the east-west axis is notably higher than across latitudes. This stability is driven by consistent trade winds, weak Coriolis forces, and uniform convergence

https://doi.org/10.5194/egusphere-2025-306
Preprint. Discussion started: 17 February 2025

zones like the ITCZ, which collectively enhance the reliability of CLCT's tropical tropospheric ozone retrievals. As a result, CLCT achieves lower bias and scatter in tropical regions compared to CLCD (Fig. 13). The CLCT algorithm also benefits from Theil-Sen regression for ACCO retrievals, avoiding large climatological corrections to the 450 hPa level in cases of high tropical clouds.

Another prominent difference in the four-year averaged TCO global maps is the high CLCD-TCO values over Central America and Northwestern Africa (Fig. 14). In Central America, this CLCD bias is likely driven by factors discussed before, including comparatively fewer ACCO measurements than CLCT and the influence of clouds from different latitudes. For Northwestern Africa, the elevated CLCD-TCO can be attributed to biomass burning activity (Jonquières et al., 1998), which releases significant amounts of ozone precursors and aerosols, reducing the accuracy of satellite ozone retrievals. Absorbing aerosols from biomass burning can introduce biases in ozone retrievals by ozone hidden below the aerosol layer (Sellitto et al., 2011; Coldewey-Egbers et al., 2005). However, since there are no ozonesonde measurements available for validation in this region, it is difficult to say whether CLCD or CLCT provides more accurate tropospheric ozone.

In terms of overall performance, the CLCT algorithm delivers a reduced bias and scatter of 0.3±1.3 DU compared to CLCD (0.8±2.8 DU) over the tropics (20°S–20°N). Consequently, for the tropics, we recommend using CLCT, given that the CLCD is primarily designed for tropospheric ozone column retrievals in the extratropics.

The CLCD algorithm outperforms CLCT at all four subtropical stations (>20°) (Hanoi, King's Park, Irene, and Reunion), demonstrating significantly reduced bias and scatter (see Table 1 and Fig. 13). In the NH, both King's Park and Hanoi exhibit similar biases of approximately -4 DU for CLCT and CLCD. However, CLCD has lower variability, with scatters of around 2 DU for Hanoi and 3 DU for King's Park, while CLCT has scatters of ∼3 DU and 5 DU, respectively. In the SH, CLCD substantially reduces bias and scatter over Irene from -2.0 ± 3.3 DU (CLCT) to 0.0±1.5 DU. At Reunion, CLCD significantly reduce the scatter (∼1 DU), compared to CLCT (∼4 DU).

6 Selected applications

The retrieval of tropospheric ozone using the CLCD algorithm provides valuable insights into atmospheric processes and air quality (pollution). In this section, we present key applications of these retrievals by examining their relationship with other trace gases such as NO_2, CO, and HCHO. They demonstrate the algorithm's capability to capture spatial patterns in tropospheric ozone and its link to anthropogenic activities, biomass burning, and precursor emissions, showcasing its utility for atmospheric research and air quality monitoring.

6.1 Enhanced tropospheric NO_2 and ozone levels over Northeast China

Figure 15 presents the spatial distribution of tropospheric ozone and NO_2 over Northeast Asia in May 2023. Elevated NO_2 concentrations are evident over the Northeast China Plain (NCP), especially around Beijing (39.9°N, 116.4°E) with corresponding high levels of tropospheric ozone. Despite low NO_2 concentrations, elevated tropospheric ozone levels are observed

https://doi.org/10.5194/egusphere-2025-306
Preprint. Discussion started: 17 February 2025

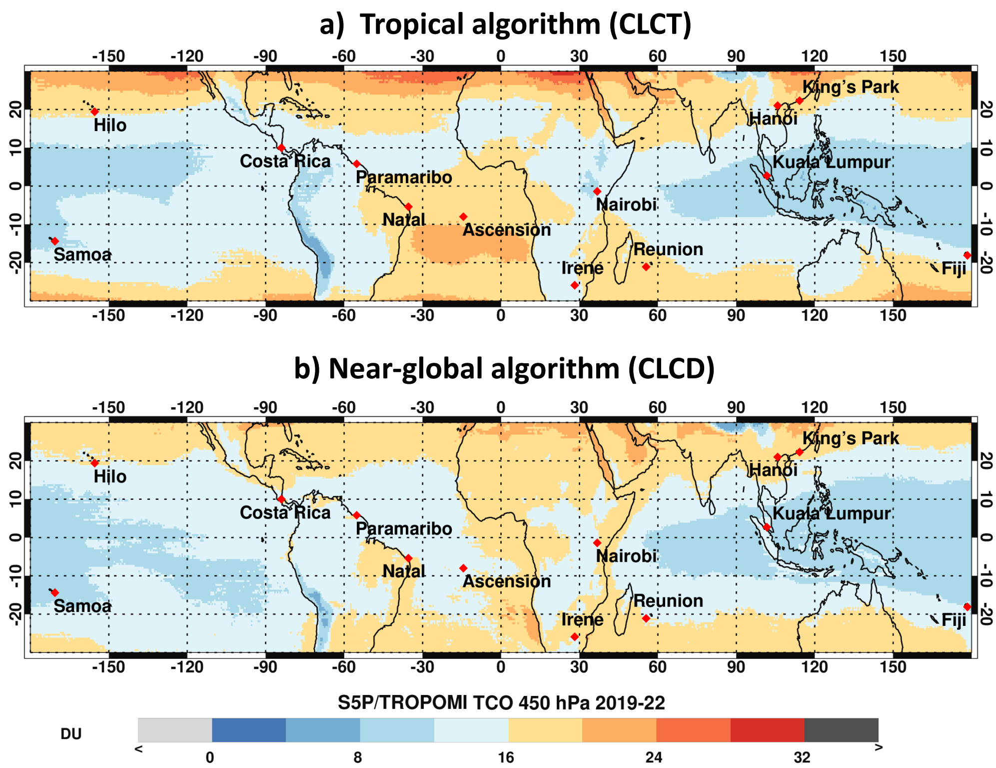

Figure 14. Global maps of a) the average tropospheric column ozone [DU] above 450 hPa retrieved using the CLCT method, and b) the CLCD method from 2019 to 2022.

in the northernmost regions, suggesting long-range transport, during which photochemical reactions further enhance ozone concentrations in the free troposphere (Zheng et al., 2021).

Summertime surface ozone levels over the Northeast China Plain rank among the highest in the northern mid-latitudes, with one of the main reasons being increased anthropogenic NO_x (including NO_2) emissions posing significant health risks in the region (Lu et al., 2018; Gaudel et al., 2018; Lu et al., 2021).

High NO_2 levels are also observed over Bangladesh (23.7°N, 90.4°E) coinciding with regional ozone enhancements, which points at its role as a precursor for ozone formation.

6.2 Impact of Canadian wildfires on ozone

Figure 16 illustrates the connection between wildfire activity (Visible Infrared Imaging Radiometer Suite, VIIRS fire count; https://firms.modaps.eosdis.nasa.gov/download/) and the enhancement of CO and tropospheric ozone.

CO is a primary product of wildfire emissions and a precursor for ozone formation. The spatial distribution of CO and ozone enhancements, especially over the upper midwest of North America, shows this connection (Fig. 16 b and c).

https://doi.org/10.5194/egusphere-2025-306
Preprint. Discussion started: 17 February 2025

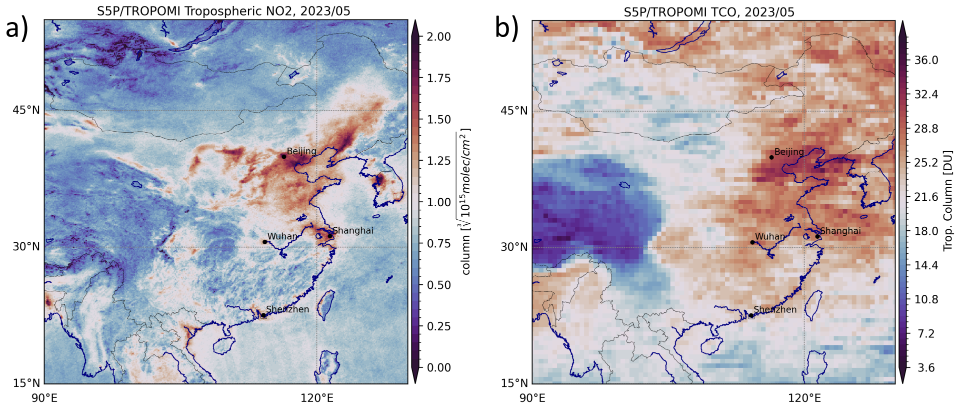

Figure 15. Monthly mean value of a) TROPOMI NO_2 and CLCD tropospheric ozone at 450 hPa over northeast Asia observed in May 2023.

As a secondary by-product, tropospheric ozone exhibits a more dispersed pattern compared to CO due to transport. Polluted air masses from wildfires rise over continents and travel across oceans and subside. During transport, interactions between NO_X from lightning and biomass burning, along with VOCs and CO, contribute to additional tropospheric ozone formation (Moxim and Levy, 2000; Heue et al., 2022).

Canadian forests, spanning 362 million hectares, faced record-breaking wildfires during the summer of 2023, burning 15 million hectares—over seven times the 40-year average (Jain et al., 2024). Inverse modelling of TROPOMI CO data estimated wildfire emissions comparable to the annual fossil fuel output of major countries like China, India, and the USA (Byrne et al., 2024). These fires also impacted regions beyond Canada, with smoke contributing to surface-level CO and ozone enhancements in the U.S. upper midwest during the summer (Cooper et al., 2024).

6.3 Formaldehyde and ozone distribution over North America

Figure 17 highlights the spatial distribution of HCHO and tropospheric ozone over North America in July 2021. High tropospheric ozone columns over North America coincide with enhanced HCHO levels, particularly in California (36.8°N, 119.4°W) and south-east of the US (38.8°N, 106.5°W). Tropospheric ozone columns show a slight spatial shift relative to HCHO, particularly towards the Pacific and the eastern U.S., due to ozone's longer atmospheric lifetime and transport by winds (Heue et al., 2022).

Formaldehyde (HCHO) is a key ozone precursor, formed from the oxidation of VOCs and NO_X, with emissions influenced by temperature, land use, and industrial activities (Millet et al., 2006). Observations from TROPOMI show the connection between summer time HCHO and ozone levels (Heue et al., 2022). Regular tropospheric ozone enhancements in the southern U.S. are attributed to VOC-rich air uplift and mixing with lightning-generated NO_X (Cooper et al., 2007; Heue et al., 2022).

https://doi.org/10.5194/egusphere-2025-306
Preprint. Discussion started: 17 February 2025

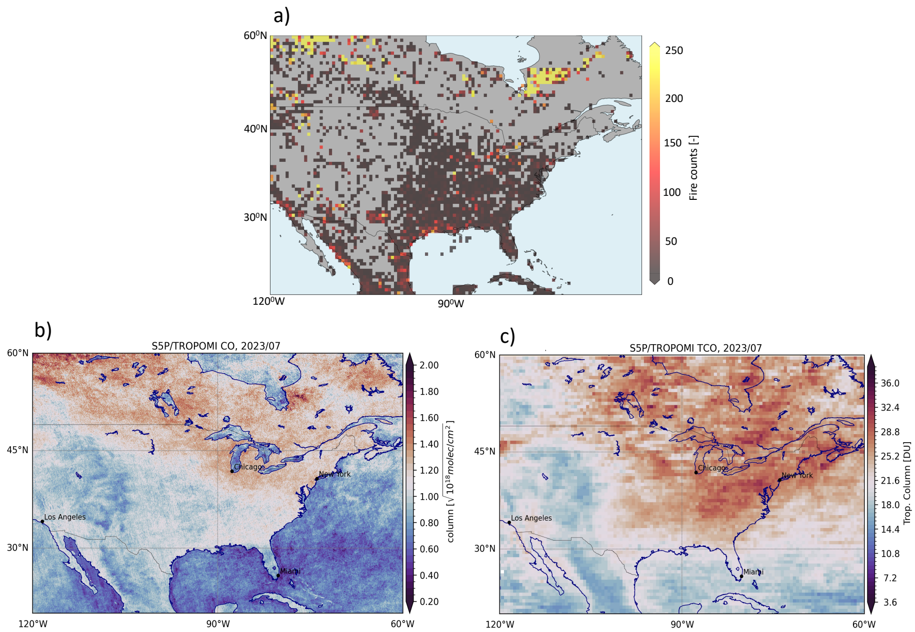

Figure 16. Monthly mean value of a) Visible Infrared Imaging Radiometer Suite (VIIRS) active fire counts, b) TROPOMI CO, and c) CLCD tropospheric ozone at 450 hPa over North America observed in July 2023.

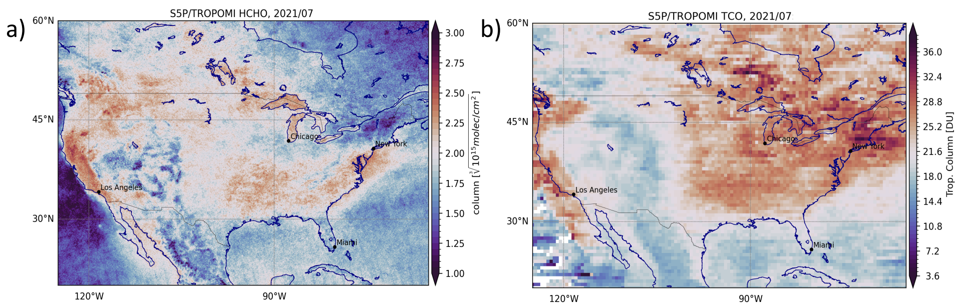

Figure 17. Monthly mean value of a) TROPOMI HCHO, and c) CLCD tropospheric ozone up to 450 hPa over North America observed in July 2021.

7 Summary and conclusions

We introduced the CLCD algorithm for tropospheric ozone retrievals in mid-latitudes (60°S–60°N). It uses a local cloud reference sector to determine the above cloud (stratospheric) ozone column. This new approach minimises the impact of complex stratospheric ozone dynamics at higher latitudes.

https://doi.org/10.5194/egusphere-2025-306
Preprint. Discussion started: 17 February 2025

The method dynamically adjusts the cloud reference sector radius, ranging from 60 to 600 km from the retrieval grid box, based on cloud coverage. It then selects either the local cloud approach employing ozone climatology (CLCD-C) or the Theil-Sen regression technique (CLCD-T) for ACCO estimation, depending on the cloud characteristics. This dual approach allows the algorithm to adapt to both homogeneous and variable cloud-top-heights, improving the accuracy of the tropospheric ozone column estimates. Additionally, the method includes a homogeneity criterion for total ozone in cloudy scenes to reduce the impact of stratospheric ozone variability.

The monthly averaged TCO values from the surface to 450 hPa, based on the CLCD algorithm, were derived from TROPOMI near-global data for the period from 2018 to 2022. The accuracy of the CLCD-TCO retrievals was evaluated by comparison with HEGIFTOM ozonesonde measurements from thirty-six globally distributed stations, which are part of the SHADOZ, WOUDC, and NDACC networks, and with our tropical algorithm CLCT (Maratt Satheesan et al., 2024).

The CLCD retrieval agrees well with ozonesondes across most stations, with an overall statistical bias of 0.6 DU and dispersion of 2.5 DU (1σ). Maximum observed bias and dispersion are well within acceptable limits, ∼5 DU and ∼4 DU, respectively. The CLCD algorithm performs well in subtropics and mid-latitudes (≥20°), effectively capturing local cloud dynamics and providing accurate retrievals.

Above ozonesonde stations experiencing complex ozone and cloud dynamics, TROPOMI tend to exhibit larger biases. This is particularly evident at high latitude stations such as Churchill (bias of ∼+5 DU) in the NH and Macquarie Island (bias of ∼+5 DU) in the SH.

For tropical regions (20°S-20°N), we recommend the CLCT algorithm (overall bias of 0.2 ± 1.4 DU) over the CLCD algorithm (0.8 ± 2.8 DU) due to its better performance. The CLCT algorithm's latitudinally confined, longitudinally varying large cloud reference sector is more appropriate in the tropics. In regions with high ozone variability, such as Kuala Lumpur, the circular reference sector used in CLCD proves more effective by incorporating more local clouds in ACCO estimation. This localized approach reduces the bias to -1.6 DU, compared to CLCT's -2.9 DU, making CLCD more reliable in areas with significant cloud and ozone variability.

The CLCD approach effectively captures tropospheric ozone enhancements across diverse regions, including Northeast China and North America, impacted by wildfires and anthropogenic emissions, respectively. Links to key precursors like NO_2, CO and HCHO, also measured by TROPOMI, have been shown (Figs. 15 to 17)

Overall, the CLCD algorithm's robust performance in mid-latitudes and its ability to adapt to local cloud/ozone conditions make it a valuable tool for global tropospheric ozone monitoring from a single nadir-viewing instrument. The low bias and scatter observed at subtropical and mid-latitude stations compared to ozonesonde measurements underscore its efficiency. The findings from this study provide a solid foundation for the application of our algorithm to past and future UV nadir-viewing satellite instruments, in particular those of geostationary satellite missions like GEMS, TEMPO, and Sentinel-5.

Data availability. Sentinel-5 Precursor TROPOMI data can 40 be accessed through the Copernicus Open Access Hub at https://sentinels.copernicus.eu/documents/247904/2476257/Sentinel-5P-ATBD-TROPOMI-Tropospheric-Ozone.pdf/d2106102-b5c3-4d28-b752-026e3448aab2?

t=1625507455328. . The ozonesonde data are available through the following repositories: HEGIFTOM (https://hegiftom.meteo.be/datasets/ozonesondes), SHADOZ (https://doi.org/10.57721/SHADOZ-V06), NDACC (http://www.ndacc.org), and WOUDC (http://www.woudc.org), all of which provide public access under their respective data policies. The data from NASA's Fire Information for Resource Management System (FIRMS), part of NASA's Earth Observing System Data and Information System (EOSDIS), are publicly available in accordance with their data policy at https://earthdata.nasa.gov/firms

Author contributions. SMS developed the CLCD algorithm and performed TCO retrievals and validated the results with HEGIFTOM, SHADOZ, WOUDC, and NDACC ozonesonde measurements, and wrote the manuscript. Both MW and KE guided and provided expertise in developing the algorithm. All authors provided comments and feedback to the manuscript.

Competing interests. At least one of the (co-)authors is a member of the editorial board of Atmospheric Measurement Techniques.

Acknowledgements. This work was funded in large part by the Federal Ministry for Economic Affairs and Climate Action (BMWi) TROPO3-MIDLAT project, which is part of the funding programme "Development of innovative methods for the creation of earth observation-based information products". The support by the federal state of Bremen is gratefully acknowledged. This work uses Copernicus Sentinel-5 Precursor reprocessed/offline satellite data (2018–2022), total ozone and cloud products processed by the European Space Agency (ESA). The ozonesonde data were obtained from these key sources: Harmonization and Evaluation of Ground-based Instruments for Free Tropospheric Ozone Measurements (HEGIFTOM, https://hegiftom.meteo.be/datasets/ozonesondes), the Network for the Detection of Atmospheric Composition Change (NDACC, http://www.ndacc.org), the World Ozone and Ultraviolet Radiation Data Centre (WOUDC, http://www.woudc.org), and NASA's Southern Hemisphere Additional Ozonesondes (SHADOZ, https://doi.org/10.57721/SHADOZ-V06). We thank the principal investigators and staff at the ozonesonde stations for their dedicated efforts in maintaining high-quality measurements and valuable scientific contributions. We gratefully acknowledge NASA's Fire Information for Resource Management System (FIRMS) for providing data utilized in this study. FIRMS is part of NASA's Earth Observing System Data and Information System (EOSDIS, https://earthdata.nasa.gov/firms, last accessed:) The calculations for this research were conducted using IDL version 8.5.1.

References

Byrne, B., Liu, J., Bowman, K. W., Pascolini-Campbell, M., Chatterjee, A., Pandey, S., Miyazaki, K., van der Werf, G. R., Wunch, D., Wennberg, P. O., et al.: Carbon emissions from the 2023 Canadian wildfires, Nature, 633, 835–839, https://doi.org/doi.org/10.1038/s41586-024-07878-z, 2024.

Coldewey-Egbers, M., Weber, M., Lamsal, L. d., De Beek, R., Buchwitz, M., and Burrows, J.: Total ozone retrieval from GOME UV spectral data using the weighting function DOAS approach, Atmospheric Chemistry and Physics, 5, 1015–1025, https://doi.org/10.5194/acp-5-1015-2005, 2005.

Cooper, O. R., Trainer, M., Thompson, A., Oltmans, S., Tarasick, D., Witte, J., Stohl, A., Eckhardt, S., Lelieveld, J., Newchurch, M., et al.: Evidence for a recurring eastern North America upper tropospheric ozone maximum during summer, Journal of Geophysical Research: Atmospheres, 112, https://doi.org/10.1029/2007JD008710, 2007.

Cooper, O. R., Parrish, D., Ziemke, J., Balashov, N., Cupeiro, M., Galbally, I., Gilge, S., Horowitz, L., Jensen, N., Lamarque, J.-F., et al.: Global distribution and trends of tropospheric ozone: An observation-based review, Elementa, 2, 000029, https://doi.org/10.12952/journal.elementa.000029, 2014.

Cooper, O. R., Chang, K.-L., Bates, K., Brown, S. S., Chace, W. S., Coggon, M. M., Gorchov Negron, A. M., Middlebrook, A. M., Peischl, J., Piasecki, A., et al.: Early Season 2023 Wildfires Generated Record-Breaking Surface Ozone Anomalies Across the US Upper Midwest, Geophysical Research Letters, 51, e2024GL111481, https://doi.org/10.1029/2024GL111481, 2024.

Crutzen, P. J.: Geology of mankind, in: Paul J. Crutzen: A pioneer on atmospheric chemistry and climate change in the Anthropocene, pp. 211–215, Springer, https://doi.org/10.1007/978-3-319-27460-7_10, 2016.

Dam, D. A., Nguyen, T. K. O., et al.: Photochemical smog introduction and episode selection for the ground-level ozone in Hanoi, Vietnam, VNU Journal of Science: Earth and Environmental Sciences, 24, http://repository.vnu.edu.vn/handle/11126/5022, 2008.

ESA: S5P/TROPOMI Total Ozone ATBD, Technical note S5P-L2-DLR-ATBD-400A, ESA, https://sentinel.esa.int/documents/247904/2476257/Sentinel-5P-TROPOMI-ATBD-Total-Ozone, 2022.

Fahey, D. W. and Hegglin, M. I.: Twenty questions and answers about the ozone layer: 2010 update, Scientific assessment of ozone depletion, pp. 4–1, 2010.

Fishman, J., Brackftt, V., and Fakhruzzaman, K.: Distribution of tropospheric ozone in the tropics from satellite and ozonesonde measurements, Journal of atmospheric and terrestrial physics, 54, 589–597, https://doi.org/10.1016/0021-9169(92)90099-7, 1992.

Gaudel, A., Cooper, O. R., Ancellet, G., Barret, B., Boynard, A., Burrows, J., Clerbaux, C., Coheur, P.-F., Cuesta, J., Cuevas, E., et al.: Tropospheric Ozone Assessment Report: Present-day distribution and trends of tropospheric ozone relevant to climate and global atmospheric chemistry model evaluation, Elementa: science of the anthropocene, 6, 2018.

Greenslade, J. W., Alexander, S. P., Schofield, R., Fisher, J. A., and Klekociuk, A. K.: Stratospheric ozone intrusion events and their impacts on tropospheric ozone in the Southern Hemisphere, Atmospheric Chemistry and Physics, 17, 10269–10290, https://doi.org/10.5194/acp-17-10269-2017, 2017.

Heue, K.-P., Coldewey-Egbers, M., Delcloo, A., Lerot, C., Loyola, D., Valks, P., and Van Roozendael, M.: Trends of tropical tropospheric ozone from 20 years of European satellite measurements and perspectives for the Sentinel-5 Precursor, Atmospheric Measurement Techniques, 9, 5037–5051, https://doi.org/10.5194/amt-9-5037-2016, 2016.

https://doi.org/10.5194/egusphere-2025-306
Preprint. Discussion started: 17 February 2025

Heue, K.-P., Loyola, D., Romahn, F., Zimmer, W., Chabrillat, S., Errera, Q., Ziemke, J., and Kramarova, N.: Tropospheric ozone retrieval by a combination of TROPOMI/S5P measurements with BASCOE assimilated data, Atmospheric Measurement Techniques, 15, 5563–5579, 2022.

Hu, Y., Yan, H., Zhang, X., Gao, Y., Zheng, X., and Liu, X.: Study on calculation and validation of tropospheric ozone by ozone monitoring instrument–microwave limb sounder over China, International Journal of Remote Sensing, 41, 9101–9120, https://doi.org/10.1080/01431161.2020.1800124, 2020.

Huang, G., Liu, X., Chance, K., Yang, K., Bhartia, P. K., Cai, Z., Allaart, M., Ancellet, G., Calpini, B., Coetzee, G. J., et al.: Validation of 10-year SAO OMI Ozone Profile (PROFOZ) product using ozonesonde observations, Atmospheric Measurement Techniques, 10, 2455–2475, https://doi.org/10.5194/amt-10-2455-2017, 2017.

Hubert, D., Lambert, J.-C., Verhoelst, T., Granville, J., Keppens, A., Baray, J.-L., Bourassa, A. E., Cortesi, U., Degenstein, D. A., Froidevaux, L., et al.: Ground-based assessment of the bias and long-term stability of 14 limb and occultation ozone profile data records, Atmospheric measurement techniques, 9, 2497–2534, https://doi.org/10.5194/amt-9-2497-2016, 2016.

Hubert, D., Heue, K.-P., Lambert, J.-C., Verhoelst, T., Allaart, M., Compernolle, S., Cullis, P. D., Dehn, A., Félix, C., Johnson, B. J., et al.: TROPOMI tropospheric ozone column data: geophysical assessment and comparison to ozonesondes, GOME-2B and OMI, Atmospheric Measurement Techniques, 14, 7405–7433, https://doi.org/10.5194/amt-14-7405-2021, 2021.

Ingmann, P., Veihelmann, B., Langen, J., Lamarre, D., Stark, H., and Courrèges-Lacoste, G. B.: Requirements for the GMES Atmosphere Service and ESA's implementation concept: Sentinels-4/-5 and-5p, Remote Sensing of Environment, 120, 58–69, https://doi.org/10.1016/j.rse.2012.01.023, 2012.

Jaffe, D. A., Cooper, O. R., Fiore, A. M., Henderson, B. H., Tonnesen, G. S., Russell, A. G., Henze, D. K., Langford, A. O., Lin, M., and Moore, T.: Scientific assessment of background ozone over the US: Implications for air quality management, Elementa: Science of the Anthropocene, 6, https://doi.org/10.1525/elementa.309, 2018.

Jain, P., Barber, Q. E., Taylor, S., Whitman, E., Acuna, D. C., Boulanger, Y., Chavardès, R. D., Chen, J., Englefield, P., Flannigan, M., et al.: Canada Under Fire–Drivers and Impacts of the Record-Breaking 2023 Wildfire Season, Authorea Preprints, https://doi.org/10.22541/essoar.170914412.27504349/v2, 2024.

Jenkins, G. S., Ndiaye, S., Gueye, M., Fitzhugh, R., Smith, J. W., and Kebe, A.: Lower/middle tropospheric ozone variability in Senegal during pre-monsoon and monsoon periods of summer 2008: observations and model results, Journal of Atmospheric Chemistry, 69, 273–302, https://doi.org/10.1007/s10874-012-9240-7, 2012.

Jensen, A. A., Thompson, A. M., and Schmidlin, F.: Classification of Ascension Island and Natal ozonesondes using self-organizing maps, Journal of Geophysical Research: Atmospheres, 117, https://doi.org/10.1029/2011JD016573, 2012.

Jonquières, I., Marenco, A., Maalej, A., and Rohrer, F.: Study of ozone formation and transatlantic transport from biomass burning emissions over West Africa during the airborne Tropospheric Ozone Campaigns TROPOZ I and TROPOZ II, Journal of Geophysical Research: Atmospheres, 103, 19 059–19 073, https://doi.org/10.1029/98JD00819, 1998.

Keppens, A., Di Pede, S., Hubert, D., Lambert, J.-C., Veefkind, P., Sneep, M., De Haan, J., ter Linden, M., Leblanc, T., Compernolle, S., et al.: Five years of Sentinel-5p TROPOMI operational ozone profiling and geophysical validation using ozonesonde and lidar ground-based networks, Atmospheric Measurement Techniques Discussions, 2024, 1–43, https://doi.org/10.5194/amt-17-3969-2024, 2024.

Leventidou, E., Eichmann, K.-U., Weber, M., and Burrows, J. P.: Tropical tropospheric ozone columns from nadir retrievals of GOME-1/ERS-2, SCIAMACHY/Envisat, and GOME-2/MetOp-A (1996–2012), Atmospheric Measurement Techniques, 9, 3407–3427, https://doi.org/10.5194/amt-9-3407-2016, 2016.

Leventidou, E., Weber, M., Eichmann, K.-U., Burrows, J. P., Heue, K.-P., Thompson, A. M., and Johnson, B. J.: Harmonisation and trends of 20-year tropical tropospheric ozone data, Atmospheric Chemistry and Physics, 18, 9189–9205, https://doi.org/10.5194/acp-18-9189-2018, 2018.

Liao, Z., Ling, Z., Gao, M., Sun, J., Zhao, W., Ma, P., Quan, J., and Fan, S.: Tropospheric ozone variability over Hong Kong based on recent 20 years (2000–2019) ozonesonde observation, Journal of Geophysical Research: Atmospheres, 126, e2020JD033 054, https://doi.org/10.1029/2020JD033054, 2021.

Loyola, D. and Ruppert, T.: A new PMD cloud-recognition algorithm for GOME, ESA Earth Observation Quarterly, 58, 45–47, https://elib.dlr.de/53/, 1998.

Lu, X., Hong, J., Zhang, L., Cooper, O. R., Schultz, M. G., Xu, X., Wang, T., Gao, M., Zhao, Y., and Zhang, Y.: Severe surface ozone pollution in China: a global perspective, Environmental Science & Technology Letters, 5, 487–494, https://doi.org/10.1021/acs.estlett.8b00366, 2018.

Lu, X., Ye, X., Zhou, M., Zhao, Y., Weng, H., Kong, H., Li, K., Gao, M., Zheng, B., Lin, J., et al.: The underappreciated role of agricultural soil nitrogen oxide emissions in ozone pollution regulation in North China, Nature Communications, 12, 5021, https://doi.org/10.1038/s41467-021-25147-9, 2021.

Ludewig, A., Kleipool, Q., Bartstra, R., Landzaat, R., Leloux, J., Loots, E., Meijering, P., van der Plas, E., Rozemeijer, N., Vonk, F., et al.: In-flight calibration results of the TROPOMI payload on board the Sentinel-5 Precursor satellite, Atmospheric Measurement Techniques, 13, 3561–3580, https://doi.org/10.5194/amt-13-3561-2020, 2020.

Maratt Satheesan, S., Eichmann, K.-U., Burrows, J. P., Weber, M., Stauffer, R., Thompson, A. M., and Kollonige, D.: Improved convective cloud differential (CCD) tropospheric ozone from S5P-TROPOMI satellite data using local cloud fields, Atmospheric Measurement Techniques, 17, 6459–6484, https://doi.org/10.5194/amt-17-6459-2024, 2024.

McPeters, R., Logan, J., and Labow, G.: Ozone climatological profiles for version 8 TOMS and SBUV retrievals, in: AGU Fall Meeting Abstracts, vol. 2003, pp. A21D–0998, 2003.

Millet, D. B., Jacob, D. J., Turquety, S., Hudman, R. C., Wu, S., Fried, A., Walega, J., Heikes, B. G., Blake, D. R., Singh, H. B., et al.: Formaldehyde distribution over North America: Implications for satellite retrievals of formaldehyde columns and isoprene emission, Journal of Geophysical Research: Atmospheres, 111, https://doi.org/10.1029/2005JD006853, 2006.

Moeini, O., Tarasick, D. W., McElroy, C. T., Liu, J., Osman, M. K., Thompson, A. M., Parrington, M., Palmer, P. I., Johnson, B., Oltmans, S. J., et al.: Estimating wildfire-generated ozone over North America using ozonesonde profiles and a differential back trajectory technique, Atmospheric Environment: X, 7, 100 078, https://doi.org/10.1016/j.aeaoa.2020.100078, 2020.

Moxim, W. and Levy, H.: A model analysis of the tropical South Atlantic Ocean tropospheric ozone maximum: The interaction of transport and chemistry, Journal of Geophysical Research: Atmospheres, 105, 17 393–17 415, https://doi.org/10.1029/2000JD900175, 2000.

Newton, R., Vaughan, G., Ricketts, H., Pan, L., Weinheimer, A., and Chemel, C.: Ozonesonde profiles from the West Pacific Warm Pool: measurements and validation, Atmospheric Chemistry and Physics, 16, 619–634, https://doi.org/10.5194/acp-16-619-2016, 2016.

Ogino, S.-Y., Miyazaki, K., Fujiwara, M., Nodzu, M. I., Shiotani, M., Hasebe, F., Matsumoto, J., Witte, J., Thompson, A. M., Nguyen-Thi, H. A., et al.: Cause of a Lower-Tropospheric High-Ozone Layer in Spring Over Hanoi, Journal of Geophysical Research: Atmospheres, 127, e2021JD035 727, https://doi.org/10.1029/2021JD035727, 2022.

Pope, R. J., Rap, A., Pimlott, M. A., Barret, B., Le Flochmoen, E., Kerridge, B. J., Siddans, R., Latter, B. G., Ventress, L. J., Boynard, A., et al.: Quantifying the tropospheric ozone radiative effect and its temporal evolution in the satellite era, Atmospheric Chemistry and Physics, 24, 3613–3626, https://doi.org/10.5194/acp-24-3613-2024, 2024.

Rodriguez, D. G. L., Thomas, W., Livschitz, Y., Ruppert, T., Albert, P., and Hollmann, R.: Cloud properties derived from GOME/ERS-2 backscatter data for trace gas retrieval, IEEE Transactions on Geoscience and Remote Sensing, 45, 2747–2758, https://doi.org/10.1109/TGRS.2007.901043, 2007.

Sellitto, P., Del Frate, F., Solimini, D., and Casadio, S.: Tropospheric ozone column retrieval from ESA-Envisat SCIAMACHY nadir UV/VIS radiance measurements by means of a neural network algorithm, IEEE transactions on geoscience and remote sensing, 50, 998–1011, https://doi.org/10.1109/TGRS.2011.2163198, 2011.

Smit, H. and Thompson, A.: the ASOPOS 2.0 Panel: Ozonesonde Measurement Principles and Best Operational Practices, WMO Global Atmosphere Watch Report Series, No. 268, World Meteorological Organization, Geneva, https://library. wmo. int/idurl/4/57720 (last access: 8 January 2024), https://library.wmo.int/idurl/4/57720, 2021.

Sofieva, V. F., Hänninen, R., Sofiev, M., Szeląg, M., Lee, H. S., Tamminen, J., and Retscher, C.: Synergy of using nadir and limb instruments for tropospheric ozone monitoring (SUNLIT), Atmospheric Measurement Techniques, 15, 3193–3212, https://doi.org/10.5194/amt-15-3193-2022, 2022.

Sonkaew, T. and Macatangay, R.: Determining relationships and mechanisms between tropospheric ozone column concentrations and tropical biomass burning in Thailand and its surrounding regions, Environmental Research Letters, 10, 065 009, https://doi.org/10.1088/1748-9326/10/6/065009, 2015.

Sterling, C. W., Johnson, B. J., Oltmans, S. J., Smit, H. G., Jordan, A. F., Cullis, P. D., Hall, E. G., Thompson, A. M., and Witte, J. C.: Homogenizing and estimating the uncertainty in NOAA's long-term vertical ozone profile records measured with the electrochemical concentration cell ozonesonde, Atmospheric Measurement Techniques, 11, 3661–3687, https://doi.org/10.5194/amt-11-3661-2018, 2018.

Tarasick, D. W., Smit, H. G., Thompson, A. M., Morris, G. A., Witte, J. C., Davies, J., Nakano, T., Van Malderen, R., Stauffer, R. M., Johnson, B. J., et al.: Improving ECC ozonesonde data quality: Assessment of current methods and outstanding issues, https://doi.org/10.1029/2019EA000914, 2021.

Thompson, A. M., Smit, H. G., Witte, J. C., Stauffer, R. M., Johnson, B. J., Morris, G., von der Gathen, P., Van Malderen, R., Davies, J., Piters, A., et al.: Ozonesonde quality assurance: The JOSIE–SHADOZ (2017) experience, Bulletin of the American Meteorological Society, 100, 155–171, https://doi.org/10.1175/BAMS-D-17-0311.1, 2019.

Thompson, A. M., Stauffer, R. M., Wargan, K., Witte, J. C., Kollonige, D. E., and Ziemke, J. R.: Regional and seasonal trends in tropical ozone from SHADOZ profiles: Reference for models and satellite products, Journal of Geophysical Research: Atmospheres, 126, e2021JD034 691, https://doi.org/10.1029/2021JD034691, 2021.

Valks, P., Koelemeijer, R., Van Weele, M., Van Velthoven, P., Fortuin, J., and Kelder, H.: Variability in tropical tropospheric ozone: Analysis with Global Ozone Monitoring Experiment observations and a global model, Journal of Geophysical Research: Atmospheres, 108, https://doi.org/10.1029/2002JD002894, 2003.

Valks, P., Hao, N., Gimeno Garcia, S., Loyola, D., Dameris, M., Jöckel, P., and Delcloo, A.: Tropical tropospheric ozone column retrieval for GOME-2, Atmospheric Measurement Techniques, 7, 2513–2530, https://doi.org/10.5194/amt-7-2513-2014, 2014.

Wai, K. M., Wu, S., Kumar, A., and Liao, H.: Seasonal variability and long-term evolution of tropospheric composition in the tropics and Southern Hemisphere, Atmospheric Chemistry and Physics, 14, 4859–4874, https://doi.org/10.5194/acp-14-4859-2014, 2014.

Weber, M., Dikty, S., Burrows, J. P., Garny, H., Dameris, M., Kubin, A., Abalichin, J., and Langematz, U.: The Brewer-Dobson circulation and total ozone from seasonal to decadal time scales, Atmospheric Chemistry and Physics, 11, 11 221–11 235, https://doi.org/10.5194/acp-11-11221-2011, 2011.

Williams, R. S., Hegglin, M. I., Kerridge, B. J., Jöckel, P., Latter, B. G., and Plummer, D. A.: Characterising the seasonal and geographical variability in tropospheric ozone, stratospheric influence and recent changes, Atmospheric Chemistry and Physics, 19, 3589–3620, https://doi.org/10.5194/acp-19-3589-2019, 2019.

Yonemura, S., Tsuruta, H., Kawashima, S., Sudo, S., Peng, L. C., Fook, L. S., Johar, Z., and Hayashi, M.: Tropospheric ozone climatology over Peninsular Malaysia from 1992 to 1999, Journal of Geophysical Research: Atmospheres, 107, ACH–1, https://doi.org/10.1029/2001JD000993, 2002.

Zheng, Y., Jiang, F., Feng, S., Cai, Z., Shen, Y., Ying, C., Wang, X., and Liu, Q.: Long-range transport of ozone across the eastern China seas: a case study in coastal cities in southeastern China, Science of the Total Environment, 768, 144 520, https://doi.org/10.1016/j.scitotenv.2020.144520, 2021.

Ziemke, J., Chandra, S., and Bhartia, P.: Two new methods for deriving tropospheric column ozone from TOMS measurements: Assimilated UARS MLS/HALOE and convective-cloud differential techniques, Journal of Geophysical Research: Atmospheres, 103, 22 115–22 127, https://doi.org/10.1029/98JD01567, 1998.

Ziemke, J., Chandra, S., and Bhartia, P.: A 25-year data record of atmospheric ozone in the Pacific from Total Ozone Mapping Spectrometer (TOMS) cloud slicing: Implications for ozone trends in the stratosphere and troposphere, Journal of Geophysical Research: Atmospheres, 110, https://doi.org/10.1029/2004JD005687, 2005.

Ziemke, J., Chandra, S., Oman, L., and Bhartia, P.: A new ENSO index derived from satellite measurements of column ozone, Atmospheric Chemistry and Physics, 10, 3711–3721, https://doi.org/10.5194/acp-10-3711-2010, 2010.

Ziemke, J. R. and Chandra, S.: Development of a climate record of tropospheric and stratospheric column ozone from satellite remote sensing: evidence of an early recovery of global stratospheric ozone, Atmospheric Chemistry and Physics, 12, 5737–5753, https://doi.org/10.5194/acp-12-5737-2012, 2012.

Ziemke, J. R., Chandra, S., and Bhartia, P. K.: "Cloud Slicing": A New Technique to Derive Upper Tropospheric Ozone from Satellite Measurements, Journal of Geophysical Research: Atmospheres, 106, 9853–9867, https://doi.org/10.1029/2000JD900768, 2001.